EFFECT OF UPSTREAM DISTURBANCES ON THE RATE OF HEAT TRANSFER FROM A SHORT SECTION OF HEATED PIPE

by

AZIMUDDIN AHMAD FARUQUI

A THESIS

submitted to

OREGON STATE COLLEGE

in partial fulfillment of the requirements for the degree of

MASTER OF SCIENCE

June 1959

APPROVED:

Redacted for Privacy

Professor of Chemical Engineering

In Charge of Major

Redacted for Privacy

Head of Department of Chemical Engineering

Redacted for Privacy

Chairman of School Graduate Committee

Redacted for Privacy

Dean of Graduate School

Date thesis is presented May 15, 1959

Typed by Betty Bryant

ACKNOWLEDGEMENTS

The author wishes to express his appreciation to Dr. James G. Knudsen for his encouragement and assistance during the course of the present study, to Mr. R. C. Mang for performing the more intricate machining work, and to the Department of Chemical Engineering for the use of its facilities.

TABLE OF CONTENTS

LIST OF FIGURES

LIST OF TABLES

EFFECT OF UPSTREAM DISTURBANCES ON THE RATE OF HEAT TRANSFER FROM A SHORT SECTION OF HEATED PIPE

CHAPTER I

INTRODUCTION

Tubular heat exchangers are widely used in industry for transferring heat from one fluid flowing inside pipes to another flowing outside them. One step in designing tubular heat exchangers is the calculation of the tube side heat transfer coefficient. A number of satisfactory equations have been presented for calculating this heat transfer coefficient for flow in long sections of heated pipe.

Many of the usual equations, however, do not adequately account for entrance disturbances, or the fact that only a short section of a tube may be heated. Often heat exchangers are built up of short tubes in which the length to diameter ratio is small and therefore the heat transfer coefficient varies considerably over the whole heated section. There, also, may be applications in which extremely short sections of the tubes will be heated and comparatively little information is available for predicting rates of heat transfer from such short heated sections as affected by the upstream disturbances and/or length of the heated section.

The present investigation deals with the rate of heat transfer from a short section of heated pipe as influenced by the rate of flow, length of heated section, and position and shape of various types of entrance configurations.

There have been rather extensive theoretical studies made of the rates of heat transfer at the point in tubes where heat transfer begins by virtue of a stepwise change in the wall temperature. These theoretical studies give local and average heat transfer coefficients as a function of heated length based on various assumptions covering the mechanics of flow in the tube. Little experimental data has been obtained for these systems.

The data obtained from the investigation served two purposes:

(a) It gave fundamental information on heat transfer in short sections of pipe.

(b) It gave information by which the rate of heat transfer in these sections could be predicted for various types of entrances.

From this study it was possible on the basis of the actual measurement of the heat transfer coefficient to:

(a) Correlate the heat transfer data in terms of the Nusselt number as a function of the Reynolds number for the short heated sections studied.

(b) Correlate the heat transfer data for the various types of entrances in terms of the variation of the Nusselt number with the distance of the entrance from the heated section.

CHAPTER II

THEORY AND PREVIOUS WORK

As a fluid flows past a solid surface which is at a different temperature than the fluid, heat is transferred between the boundary and the fluid. The rate of heat transfer is proportional to the area of the solid boundary and the temperature difference between the boundary and the fluid. This may be expressed as

$$dq \propto dA_w \, (T_w - T_a) \qquad (1)$$

where dq: amount of heat transferred per unit time.

dA_w: area of solid over which heat transfer takes place.

T_w: temperature of the solid surface.

T_a: temperature of the fluid.

Removing the proportionality constant one obtains

$$dq = h_1 \, dA_w \, (T_w - T_a) \qquad (2)$$

where h_1 is defined as the local heat transfer coefficient between the fluid and the boundary at the particular point in question.

The value of the local heat transfer coefficient is influenced by a number of factors, namely:

(a) The physical properties of the flowing fluid.

(b) The rate of flow of the fluid.

(c) The mechanism of flow of the fluid.

(d) The geometry of the system.

(e) The method of defining the temperature difference ($T_w - T_a$).

As heat is transferred through a fluid, a temperature profile exists in the fluid and a common definition of the local heat transfer coefficient is based on T_a being the bulk temperature of the flowing fluid. This definition is employed in heat transfer in pipes. When heat transfer occurs during flow over immersed bodies T is usually taken as the temperature of the flowing fluid an infinite distance from the surface.

Regardless of the mechanism of flow of the fluid a thin film is considered to exist at the surface of the solid boundary. In this film flow is laminar and heat transfer through it is by molecular conduction alone. The rate of heat transfer, therefore, may be expressed as:

$$dq = - kdA_w \left(\frac{\partial T}{\partial y}\right)_{y=o} \qquad (3)$$

where k: the thermal conductivity of the fluid.

y: the distance measured normal to the solid surface and away from it.

$\left(\frac{\partial T}{\partial y}\right)_{y=o}$ is the temperature gradient in the fluid at the boundary. Combining equations (2) and (3) the local heat transfer coefficient is expressed in terms of the temperature gradient at the wall

$$h_i = - \frac{k}{T_w - T_a} \left(\frac{\partial T}{\partial y} \right)_{y = o} \tag{4}$$

The geometrical factors which affect the local coefficient in tubes are pipe diameter, distance from the inlet, and distance from point of beginning of heat transfer. The position of the inlet determines the degree of development of the velocity profile while the position of the beginning of heat transfer determines the development of the temperature profile in the stream. At the beginning of heat transfer, the heat transfer coefficient is infinite since at this point the temperature gradient is infinite. The heat transfer coefficient decreases beyond the point of beginning heat transfer and becomes constant some distance downstream. The length of pipe required is called the thermal entrance length.

The mechanics of flow of the flowing fluid is determined by the flow rate and configuration upstream from the heat transfer section.

By dimensional analysis, it is possible to derive the dimensionless groups by which heat transfer data may be correlated empirically. For heat transfer in a circular tube the local heat transfer coefficient at given distance x from the beginning of heating is a function of x, the tube diameter D, the fluid velocity U and the fluid physical properties such as density ρ, heat capacity C_p, viscosity μ, and thermal conductivity k. A dimensional analysis involving these variables results in

$$\frac{h_i D}{k} = \phi\left[\frac{DU\rho}{\mu}, \quad \frac{C_p \mu}{k}, \quad \frac{x}{D}\right] \tag{5}$$

where $\frac{h_i D}{k}$: the local Nusselt number, Nu_i.

$\frac{DU\rho}{\mu}$: the Reynolds number, Re.

$\frac{C_p \mu}{k}$: the Prandt number, Pr.

$\frac{x}{D}$: the ratio of the distance from the beginning of heat transfer to the pipe diameter.

Theoretical studies of the local heat transfer coefficient involve consideration of the momentum, continuity and energy equation for the fluid flow in the circular tube. Solution of these equations with given boundary conditions gives the velocity and temperature profile as a function of the space and from this information the heat transfer coefficient may be predicted. Results of these analytical studies may also be expressed in terms of the dimensionaless groups defined above.

The temperature profile and hence the temperature gradient at the wall is found from solutions of the energy equation. For two dimensional incompressible flow the energy equation is given by

$$u \frac{\partial T}{\partial x} + v \frac{\partial T}{\partial y} = \frac{k}{C_p \rho} \left[\frac{\partial^2 T}{\partial x^2} + \frac{\partial^2 T}{\partial y^2} \right] \quad (6)$$

One of the simplest solutions of this equation is that of Leveque as reported by Knudsen and Katz (7, P. 363-367). The solution is based on the following assumptions:

(a) The fluid properties are constant.

(b) The surface temperature is constant at T_w.

(c) The undisturbed fluid temperature is T_∞.

(d) Heat transfer is by conduction only.

(e) The fluid has velocity only in the x - direction given by $u = cy$.

Neglecting the term $\frac{\partial^2 T}{\partial x^2}$ in comparison with $\frac{\partial^2 T}{\partial y^2}$ equation (6) becomes

$$cy \frac{\partial T}{\partial x} = a \frac{\partial^2 T}{\partial y^2} \quad (7)$$

where $a = \frac{k}{C_p \rho}$, the thermal diffusivity

The boundary conditions are:

(a) at $x = o$ and $y > o$ $T = T_\infty$.

(b) at $x > o$ and $y = o$ $T = T_w$.

From the solution of the equation the expression for the local heat transfer coefficient is

$$h_1 = \frac{k}{0.893} \left(\frac{C}{9ax}\right)^{1/3} \tag{8}$$

Defining the average heat transfer coefficient over a heated section L feet long as

$$h = \frac{1}{L} \int_o^L h_1 \, d\, x \tag{9}$$

the following expression is obtained

$$h = \frac{1.5\ k}{0.893} \left(\frac{C}{9aL}\right)^{1/3} \tag{10}$$

For laminar flow in a circular pipe the velocity gradient is given by

$$\left(\frac{d\ u}{d\ y}\right)_{y=o} = C = \frac{4U}{r_w}$$

where r_w is the pipe radius. Substituting this expression in equation (10), the relationship becomes

$$h = \frac{1.5\ k}{0.893} \left(\frac{4\ U}{9\ r_w a\ L}\right)^{1/3} \tag{11}$$

The corresponding expression for the average Nusselt number in dimensionless groups is

$$Nu = \frac{h\ D}{K} = 1.615\ (Re)^{1/3} (Pr)^{1/3} \left(\frac{D}{L}\right)^{1/3} \tag{12}$$

For turbulent flow in a circular pipe the velocity gradient in the laminar sublayer is given by

$$\left(\frac{du}{dy}\right)_{y=o} = C = \frac{f \rho U^2}{2 \mu}$$

where f is the friction factor. Substituting this expression for C in equation (10), the relationship for h becomes

$$h = \frac{1.5k}{0.893}\left(\frac{f \rho U^2}{18a \mu L}\right)^{1/3} \qquad (13)$$

In terms of dimensionless groups the corresponding expression for the average Nusselt number is

$$Nu = \frac{1.5}{0.893}\left(\frac{f}{18}\right)^{1/3} Re^{1/3} Pr^{1/3}\left(\frac{D}{L}\right)^{1/3} \qquad (14)$$

For fully developed laminar flow in smooth circular tubes the energy equation becomes

$$u \frac{\partial T}{\partial x} = \frac{k}{C_p \rho}\left[\frac{1}{r} \frac{\partial}{\partial r}\left(r \frac{\partial T}{\partial r}\right)\right] \qquad (15)$$

assuming radial symmetry.

One of the earliest solutions for this equation was given by Graetz. The solution has been reported in detail by Jakob (5, P. 451-456) for constant wall temperature. Sellars, Tribus and Klein (11) have considered other boundary conditions and given values of constants and eigenvalues to be used in the solutions.

For turbulent flow the eddy diffusivity of heat, ε_H, has to be included in the energy equation which, then, becomes

$$u \frac{\partial T}{\partial x} = \frac{1}{r} \frac{\partial}{\partial r}\left[r\left(\frac{k}{C_p \rho} + \varepsilon_H\right)\frac{\partial T}{\partial r}\right] \qquad (16)$$

This equation also assumes radial symmetry.

Latzko (8) first gave an approximate solution of this equation for a fluid with Prandtl number of unity. He calculated values of ε_H from the assumed relationship $\frac{\varepsilon_H}{\varepsilon_M} = 1.0$ where ε_M is the eddy diffusivity of momentum and may be calculated from the friction factor and the turbulent velocity profile. The ratio $\frac{\varepsilon_H}{\varepsilon_M}$ is designated by α . For the case of uniform wall temperature and fully developed turbulent flow the expression for the local heat transfer coefficient obtained by Latzko is

$$h_1 = \frac{0.0384}{(Re)^{0.25}} \left[1 + 0.1 \exp\left(- \frac{2.7x}{(Re)^{0.25} D} \right) + 0.9 \exp\left(- \frac{29.27x}{(Re)^{0.25} D} \right) - 0.023 \exp\left(- \frac{31.96x}{(Re)^{0.25} D} \right) \right] \quad (17)$$

From this Boelter, Young and Iverson (2) obtained the following expression for the average heat transfer coefficient

$$h = h_\infty \left\{ 1 + 0.067 (Re)^{0.25} \frac{D}{L} + \frac{D}{L} (Re)^{0.25} \left[\frac{0.1}{2.7} \exp\left(- \frac{2.7L}{(Re)^{0.25} D} \right) + \frac{0.9}{29.27} \exp\left(- \frac{29.27\, L}{(Re)^{0.25} D} \right) + \frac{0.023}{31.96} \exp\left(- \frac{31.96\, L}{(Re)^{0.25} D} \right) \right] \right\} \quad (18)$$

In this equation h_∞ is the value of the heat transfer coefficient far downstream from the point where the heat transfer starts and where the temperature profile has become fully developed.

The value of h_∞ may be calculated from many existing empirical equations. One of the most commonly used ones is that of Dittus - Boelter as reported by Knudsen and Katz (7, P. 394).

$$\frac{h_\infty D}{k} = 0.023 (Re)^{0.8} (Pr)^n \tag{19}$$

The conditions for this equation are:

(a) All fluid properties evaluated at the bulk temperature.

(b) Pr between 0.7 and 100.

(c) $n = 0.4$ for heating and 0.3 for cooling.

(d) $Re > 10,000$.

(e) $L/D > 60$.

It will be noticed that in all empirical correlations of this type, the ratio L/D does not appear. Once the temperature profile is established in the flowing fluid, the heat transfer coefficient becomes constant. Only while the temperature profile is developing (i.e. for small L/D ratios) does the heat transfer coefficient vary with the L/D ratio.

Deissler (3) gave another solution of the energy equation (16). The conditions he treated are:

(a) Uniform wall temperature, uniform initial temperature distribution, fully developed velocity distribution and constant fluid properties for gases.

(b) Uniform heat flux, uniform initial velocity and temperature distribution and constant properties for gases.

(c) Uniform wall temperature, uniform initial velocity and temperature distribution and constant properties for gases.

(d) Uniform heat flux, uniform initial temperature distribution, fully developed velocity distribution and constant fluid properties for liquid metals.

For each of these conditions Deissler calculated the local Nusselt number as a function of $\frac{x}{D}$ with the Reynolds number as parameter. In solving the energy equation Deissler assumed that $\alpha = 1.0$. He presented his results graphically. For air there is very little difference between the local Nusselt number for the constant wall temperature and uniform heat flux conditions.

Boelter, Young and Iverson (2) studied heat transfer to air flowing inside heated tubes with various types of entrances. Among the entrance conditions considered were bellmouth entrances, long $\left[\frac{l}{D} = 11.2\right]$ and short $\left[\frac{l}{D} = 2.8\right]$ unheated calming sections and small $\left[\frac{D}{D_o} = 1.715\right]$ and large $\left[\frac{D}{D_o} = 1.267\right]$ orifice entrances. The bellmouth entrance gives a uniform temperature and velocity distribution of the air at the entrance. The long calming section gives a fully developed turbulent velocity and uniform temperature profile at the beginning of heat transfer.

These authors found that their results for uniform initial temperature and fully developed turbulent velocity profile gave values of h_1 that are 10 - 30 percent higher than those predicted by Latzko's equation, (17). The authors concluded that Latzko's equation is not very reliable. For all the entrance conditions they correlated their results by means of a K factor defined by the equation

$$h = h_{\infty}\left(1 + K \frac{D}{L}\right)$$

where K had a definite value for each configuration studied.

Sleicher and Tribus (13) obtained another solution of the energy equation for fully developed turbulent flow. The restrictions on the solution as given by these authors are:

(a) Fluid properties are constant.

(b) Mean velocity in axial direction is independent of angular position.

(c) Mean radial velocity is zero.

(d) Mean temperature at any radius does not vary with time or angular position.

(e) Frictional dissipation of energy is negligible.

In solving the equation the authors used values of α for any Prandtl number by multiplying Jenkins (6) values with a factor such that agreement was reached with the experimental results of Sleicher (12) for air. That is

$$\alpha(Pr) = \frac{\alpha_s (air)}{\alpha_j (air)} \alpha_j (Pr)$$

where $\alpha(Pr)$ is the value of α for any Prandtl number used by the authors in their solution and where α_j is determined from Jenkin's analysis and α_s from Sleicher's experimental measurements.

For uniform wall temperature they obtained the following expression for the local Nusselt number

$$Nu_1 = \frac{\sum_0^\infty A_n \exp(-\lambda_n^2 x_*)}{2 \sum_0^\infty \frac{A_n}{\lambda_n^2} \exp(-\lambda_n^2 x_*)} \tag{20}$$

where λ_n are eigenvalues, A_n constants and $x_* = \frac{2x}{Re\ Pr\ D}$

These authors also given values of the first three eigenvalues and constants for various Prandtl numbers and pointed out that for $\frac{x}{D} >$ about four the first three eigenvalues and constants give values of Nu_1 which agree quite well with experimental data. For values of $\frac{x}{D} <$ four more eigenvalues and constants are needed. At $x = 0$ the local heat transfer coefficient should be infinite.

However, using only the first three eigenvalues and constants a finite value of Nu_1 is obtained at $x = o$.

When x becomes large this equation (20) reduces to

$$Nu_1 = \frac{\lambda_o^2}{2} \tag{21}$$

The authors noted that for air values of the average Nusselt number obtained from this expression agreed very well with those obtained from the Dittus-Boelter equation (19). They also noted that values of Nu_1 obtained assuming uniform wall temperature were nearly the same as those obtained assuming uniform heat flux.

When a fluid flowing with an average velocity U in the x direction and zero in the y and z directions encounters a flat plate, a boundary layer forms adjacent to the plate. The thickness of the boundary layer increases with increasing values of x. Flow in the main stream may be turbulent but the flow in the boundary layer is laminar. The boundary layer and the velocity profiles are shown schematically in (Figure 1).

The energy equation (6) has also been solved for flow over flat plates. Assuming a velocity distribution in the laminar boundary layer of the form

$$\frac{u}{U} = 1.5 \frac{y}{\delta} - 1/2 \left(\frac{y}{\delta}\right)^3 \tag{22}$$

where δ is the thickness of the hydrodynamical boundary

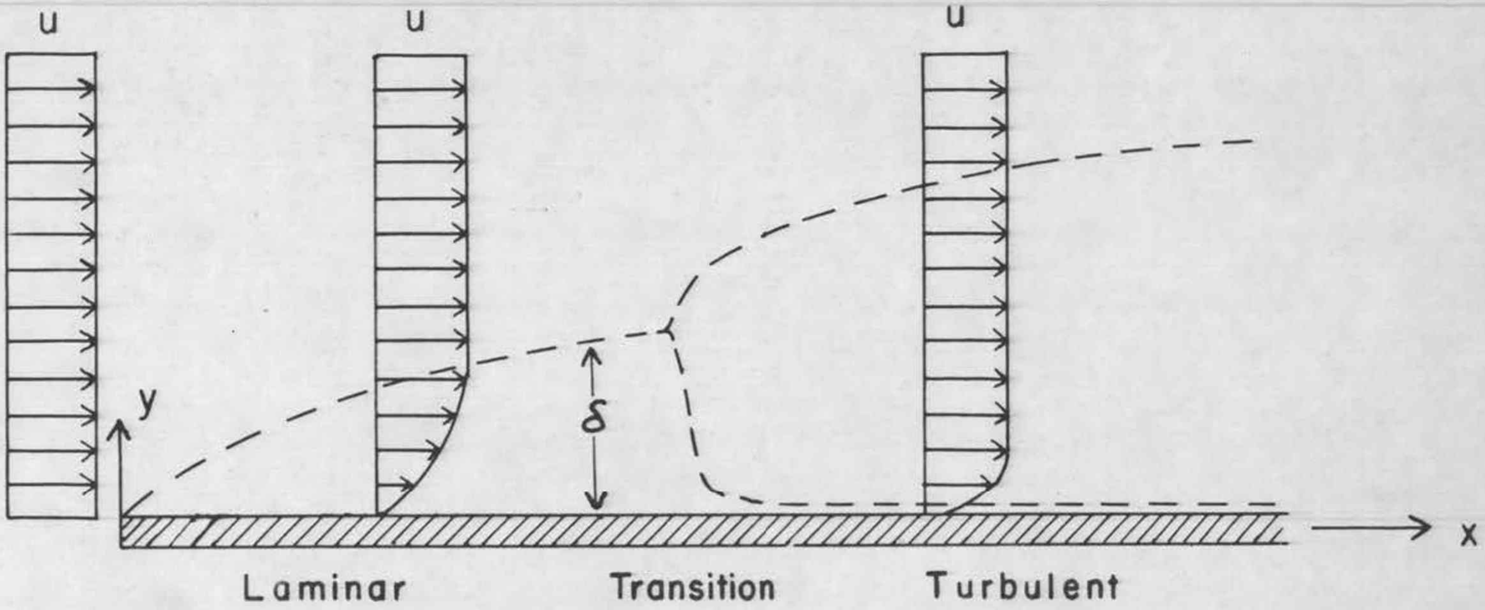

FLOW OVER A FLAT PLATE

FIGURE I

layer and assuming a temperature distribution of the same form, the following expressions are obtained. (Knudsen and Katz (7, p. 481-483).)

$$Nu_x = 0.324 \, (Re_x)^{1/2} \, (Pr)^{1/3} \tag{23}$$

$$Nu_L = 0.648 \, (Re_L)^{1/2} \, (Pr)^{1/3} \tag{24}$$

In these equations

$Nu_x = \dfrac{h_1 \; x}{k}$ the local Nusselt number for flat plates.

$Re_x = \dfrac{xU\rho}{\mu}$ the local Reynolds number for flat plates.

$Nu_L = \dfrac{h \, L}{k}$ the average Nusselt number for flat plates.

$Re_L = \dfrac{L \, U \rho}{\mu}$ the total Reynolds number for flat plates.

The conditions for the solution are

(a) Uniform wall temperature.

(b) $Pr > 0.6$.

(c) $Re_x < 300,000$.

(d) Fluid properties evaluated at $0.58 \, (T_W - T_\infty) + T_\infty$.

(e) Heating starts at leading edge.

If heating starts at a distance x_o from the leading edge equation (23) should be multiplied by the factor

$$\left[1 - \left(\frac{x_o}{x} \right)^{3/4} \right]^{-1/3}$$

As the laminar boundary layer increases in thickness it becomes unstable and the flow in it becomes turbulent. However it is assumed that a laminar sublayer exists adjacent to the wall. This is shown in (Figure 1).

Using a velocity distribution of the form

$$\frac{u}{U} = \left(\frac{y}{\delta}\right)^{1/7} \tag{25}$$

and a temperature distribution of the same form in the turbulent boundary layer the following expressions for the local and average Nusselt numbers are obtained (Knudsen and Katz (7, P. 485).)

$$Nu_x = 0.0292\ (Re_x)^{4/5} \tag{26}$$

$$Nu_L = 0.0366\ (Re_L)^{4/5} \tag{27}$$

These equations are valid under the following conditions:

(a) Boundary layer turbulent over the whole plate.

(b) Heat transfer starts from the leading edge and takes place over the whole plate.

(c) Fluid properties evaluated at

$$T - \left(\frac{0.1\ Pr + 40}{Pr + 72}\right)(T_\infty - T_W)$$

(d) The wall temperature is constant.

(e) $Pr = 1.0$.

The effect of Prandtl number can be included by use of Colburn's analogy. The equations (26 and 27) should be multiplied by $(Pr)^{1/3}$. They then become valid for $Pr > 0.6$.

Eckert (4, P. 118) gives expressions for corrections to be applied to these equations if the boundary layer over the plate is both laminar and turbulent and if heating does not start from the leading edge.

The energy equation for turbulent flow heat transfer in pipes has been solved graphically by Longwell (10). The author, after transformation of coordinates, writes the two dimensional energy equation in a difference form and solves it graphically by a Schmidt type construction.

He wrote the energy equation as

$$\frac{\partial \phi}{\partial x} = f_1(r) \frac{\partial}{\partial r}\left[f_2(r) \frac{\partial \phi}{\partial r}\right] \qquad (28)$$

where $\phi = \frac{T - Ta}{T_w \; T_a}$. For turbulent flow in a pipe $f_1(r) = \frac{1}{ur}$ and $f_2(r) = r\,\bar{\varepsilon}_H$ where $\bar{\varepsilon}_H$ is the total thermal diffusivity, $\varepsilon_H + \frac{k}{C\rho}$.

A new variable, w, was defined by $dw = -\frac{dr}{f_2(r)} = -\frac{dr}{r\,\bar{\varepsilon}_H}$. A new function of w, $f_3(w)$ was introduced as follows:

$$f_3(w) = \frac{f_1(r)}{f_2(r)} = \frac{1}{ur^2\,\bar{\varepsilon}_H}$$

Substituting these in the energy equation it becomes

$$\frac{\partial \phi}{\partial x} = f_3 (w) \left(\frac{\partial^2 \phi}{\partial w^2} \right) \tag{29}$$

Like the two dimensional heat conduction equation, this equation can be solved by a Schmidt - type graphical method. However, in this case the finite increments in x and w are not independent but are constrained to satisfy the relationship

$$\frac{2 (\Delta x) \, f_3 (w_n)}{(\Delta w_{n-1}) \, (\Delta w_{n+1})} = 1 \tag{30}$$

where the subscript n refers to the nth increment in w .

An example showing the use of this method is given in appendix (1).

CHAPTER III

EXPERIMENTAL APPARATUS

The major components of the experimental apparatus were the lucite pipe with the test section, various types of entrance configurations, the power source and the heating element, thermocouples and the e.m.f. measuring equipment and the air source.

A flow diagram of the apparatus used is shown in (Figure 2).

1. Lucite Pipe and Test Section

The test section consisted of a short length of copper pipe located between two sections of lucite pipe 1 inch I.D. and 1-1/2 inch O.D. The test section was located about 50 diameters downstream from the entrance to the lucite pipe. Two different lengths of test section, one 2 inch and the other 1 inch, were used in the experiments. The test sections were made from a 1-3/4 inch diameter copper bar of the appropriate length. A 1 inch hole was drilled through the center, perpendicular to the radial axis, and 4 1/32 inch holes were drilled on the circumference to within 0.1 inch of the inside surface. Iron-constantan thermocouples were located in these holes. The test section was held between the lucite pipe sections by flanges as shown in detail in (Figure 3). When the 2 inch test section was used, 1/16

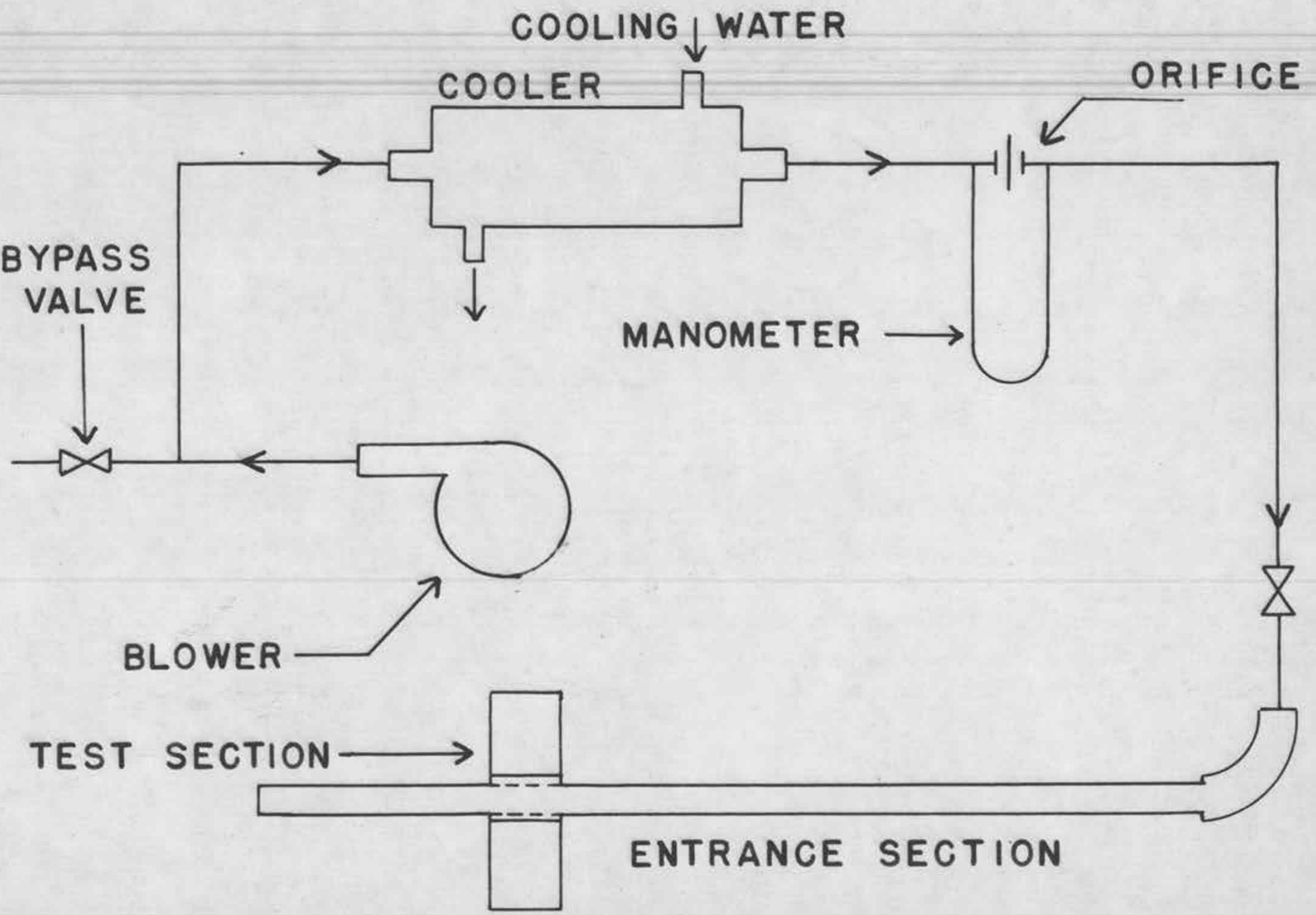

FLOW DIAGRAM OF THE APPARATUS

FIGURE 2

inch rubber gaskets were used to separate the test section from the lucite pipe. No gaskets were used with the 1 inch test section. After securing the test section in place it was honed to take out any discontinuities at the junction of the copper section and the lucite pipe. The test section was covered by a lucite box packed with vermiculite insulation to prevent heat losses. After the test section the air passed through 10 diameters of 1 inch I.D. lucite pipe and discharged into the atmosphere.

A diagramatic sketch of the test section is shown in (Figure 3).

2. Types of Entrance Configurations

Two types of disturbers - nozzles and sharp-edged orifices - were used in the entrance section. The nozzles were made from 1/2 inch thick lucite and the orifices from 1/8 inch lucite. In the experiments conducted with the 2 inch test section both orifices and nozzles with diameters of 1/2 inch and 1/4 inch were used, while with the 1 inch test section only the 1/2 inch nozzle was used.

The disturbers were machined so that they fitted snugly in the lucite pipe. The disturber to be used was placed in the entrance section of the pipe and pushed to the desired position in front of the test section by a long smooth rod. Pressure was applied on the pipe at this point by means of a

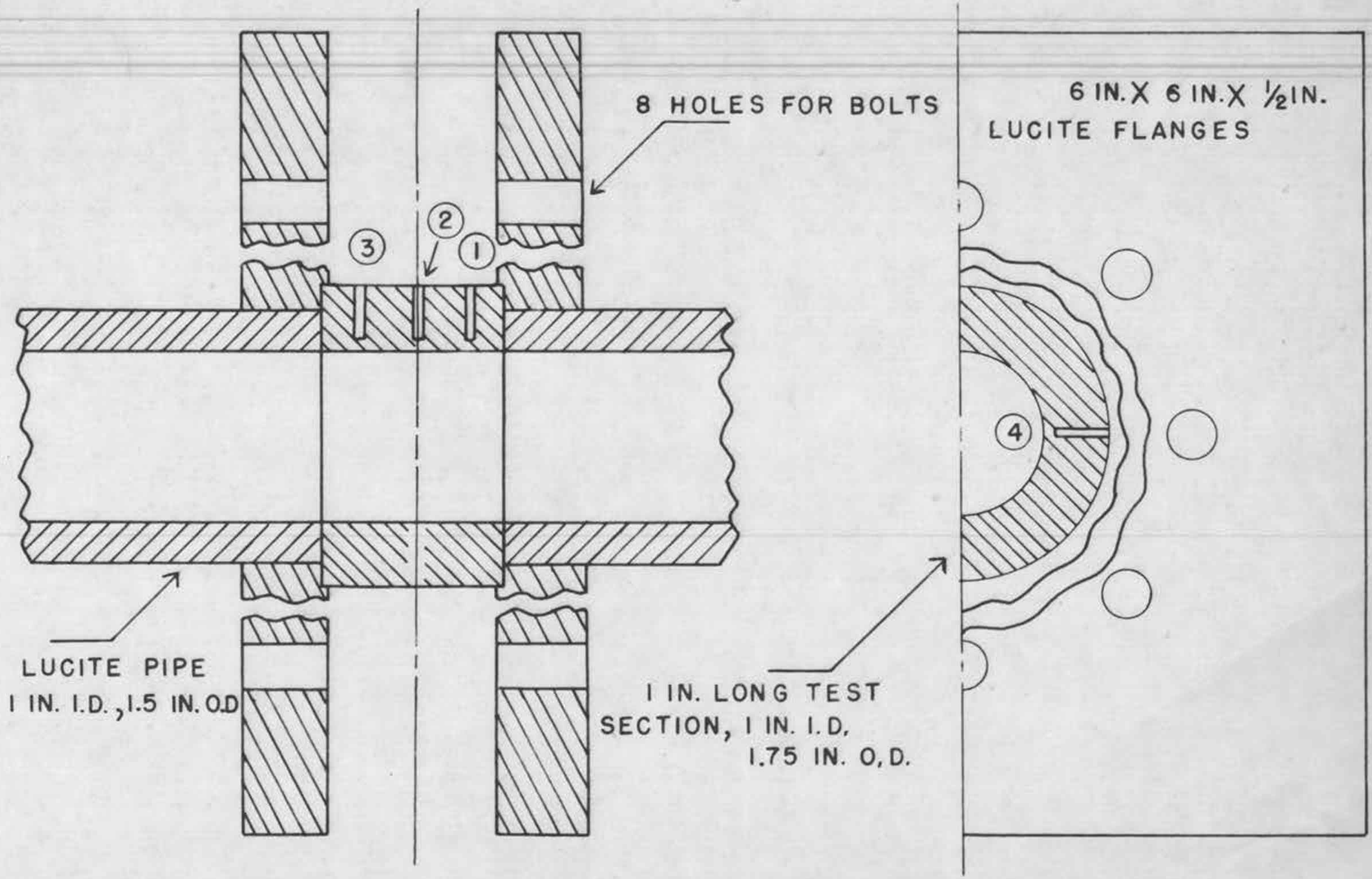

FIGURE 3 VIEWS OF TEST SECTION

clamp. Lucite compresses slightly and clamping the pipe squeezed it enough to hold the disturber securely in place.

3. Power Source and Heating Element

Heat to the test section was supplied by passing current through a 30 ga. enamelled nichrome resistance wire wound around the copper section. Power to the resistance wire was supplied by a source consisting of a voltage stabilizer and a selenium rectifier with an input of 115 volts 60 cycle A.C. and output of 130 volts D.C. The current to the resistance wire was adjusted by a variable transformer. The voltage drop across the resistance wire and the current through it were measured by a Weston Voltmeter and Ammeter with ranges of 0-150 volts (Scale: 1 division = 1 v.) and 0-1.0 amperes (Scale: 1 division = 0.001 amp.) respectively. A wiring diagram is shown in (Figure 4).

4. Thermocouples and E.M.F. Measuring Equipment

Iron-constantan thermocouples were used to measure the temperature of the incoming air and at different points on the test section. The thermocouple positions in the test section are shown in (Figure 3) and a wiring diagram of the thermocouple system is shown in (Figure 5). The cold junction was placed in cracked ice to maintain a temperature of

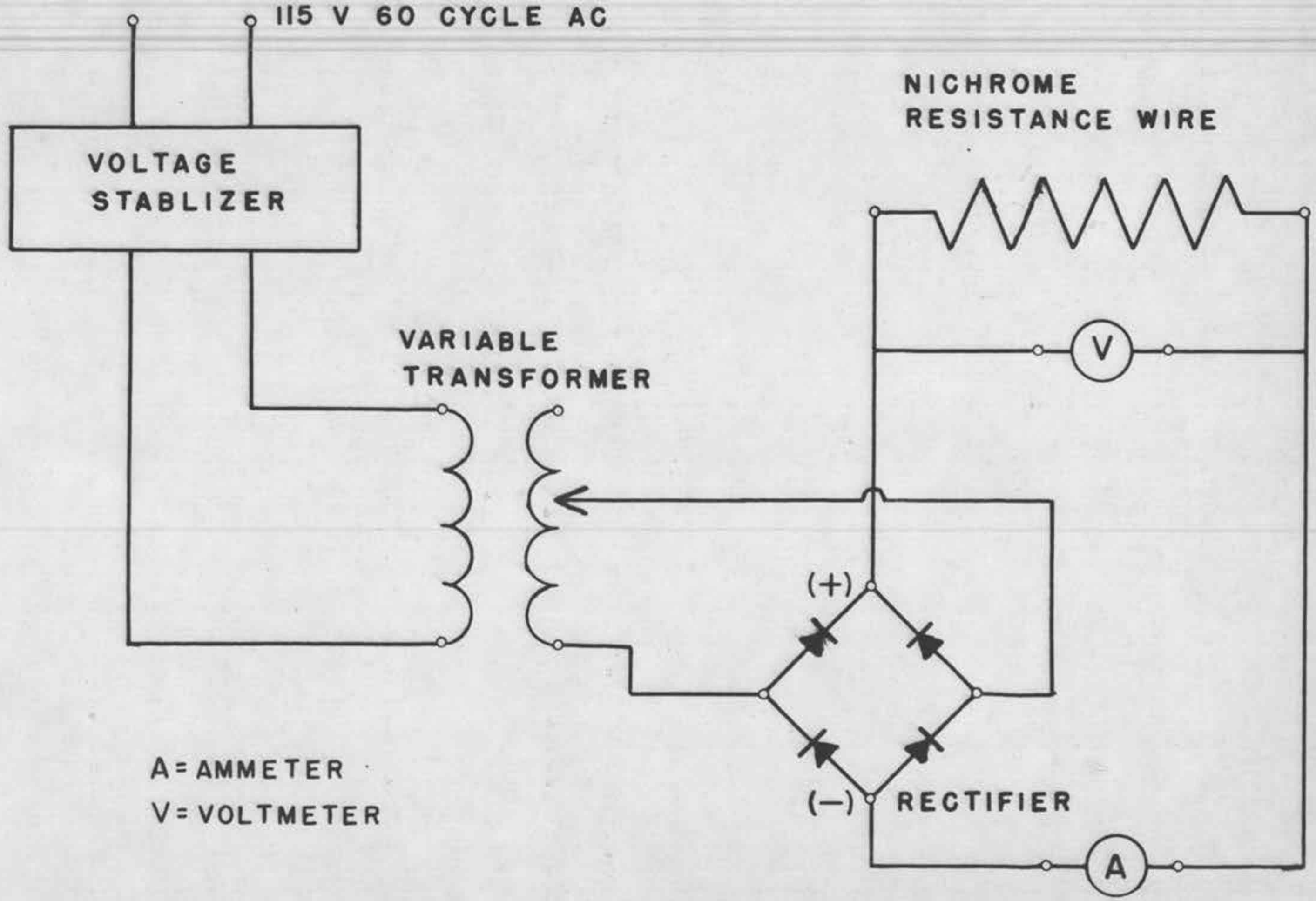

FIGURE 4 WIRING DIAGRAM FOR POWER SYSTEM

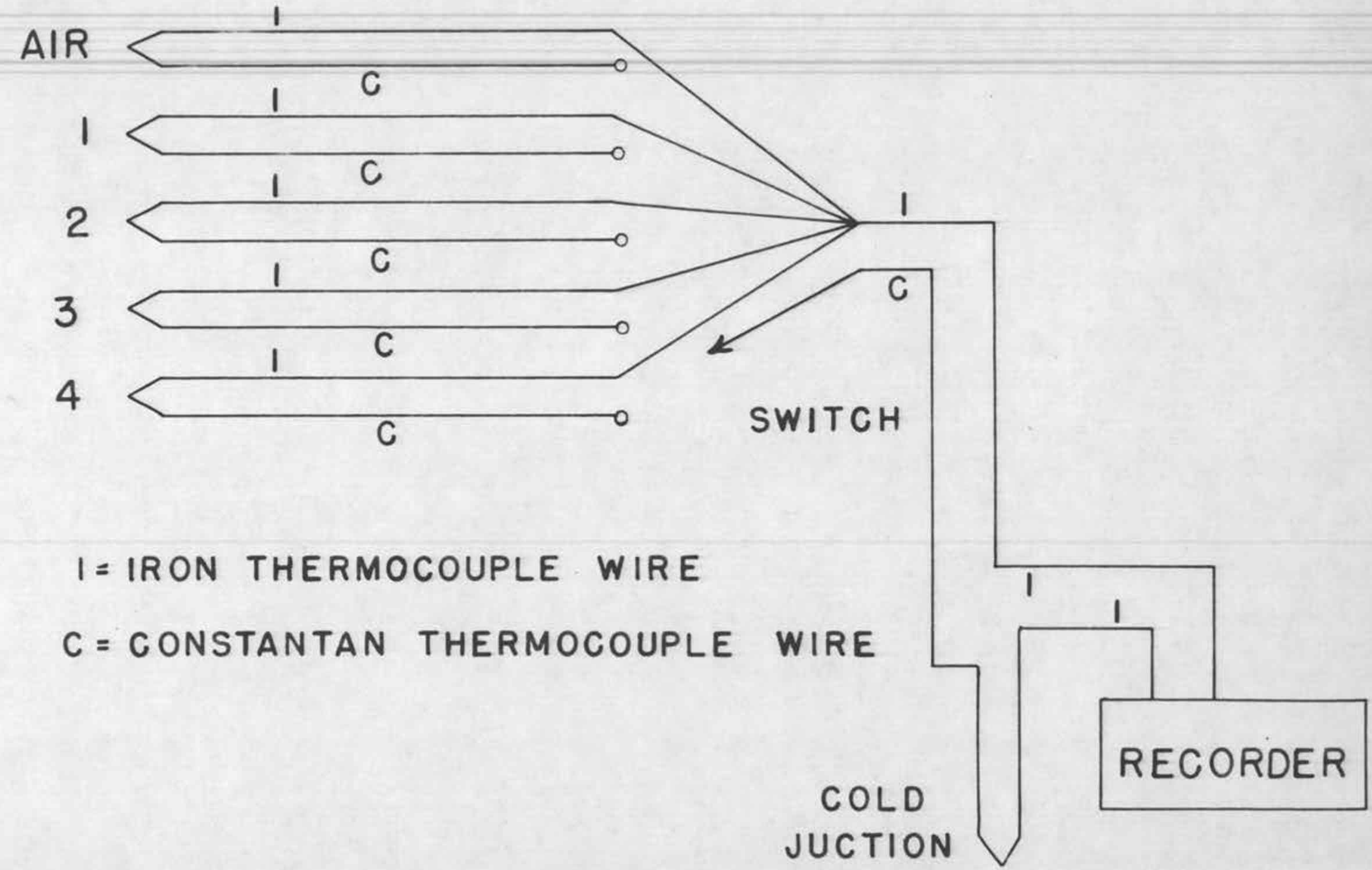

FIGURE 5 DIAGRAM OF THERMOCOUPLE SYSTEM

32° F. The voltage generated by the thermocouples was measured by a Leeds & Northrup Adjustable Zero, Adjustable Range Speedomax recorder. Tables given in the "Standard Conversion Tables for Thermocouples" (9, P. 6) were used to convert the voltage readings to the corresponding temperatures.

5. Air Source

A Roots type air blower with a rating of 280 c.f.m. at 3-1/2 p.s.i.g. was used to supply the air. After coming out of the blower, the air was cooled by water in one tubular and two finned tube box type coolers. The air then passed through a sharp-edged orifice used to measure its flow rate. The pressure drop across the orifice was measured by a manometer containing a fluid of 0.83 specific gravity. Ambrose's (1, P. 166) calibration curves for the orifices were used. The calibration was checked with a gas meter. It was found that the flow rate calculated from the orifice manometer was about 3% more than the flow rate read on the meter. An appropriate correction was made in the calculations. The pressure at the orifice was measured and it was assumed that the pressure at the test section was atmospheric.

CHAPTER IV

EXPERIMENTAL PROGRAM AND PROCEDURE

Data were taken for two different lengths of the test section, both with and without disturbers in the entrance section. The maximum flow rate obtained was governed by the maximum pressure drop permissible across the apparatus and the minimum flow rate was governed by the desired accuracy in reading the orifice manometer deflection at low pressure differentials.

Table (1) gives a resumé of all the data taken. It gives the Reynolds number range studied for all the disturbers and test sections. It also gives the disturber positions studied. This position gives the distance between the downstream end of the disturber and the upstream end of the test section and is given the symbol ℓ .

To calculate the flow rate, the orifice size, the orifice manometer deflection, the pressure at the orifice, the air temperature and the atmospheric pressure were needed.

The steady state temperature of the test section was read by the thermocouples at the positions shown in (Figure 3). An average of the four readings was used as the average wall temperature of the test section. The heat transfer coefficient was calculated by an energy balance

<u>TABLE 1</u>

<u>Summary of Experimental Program</u>

Group No.	Test Section	Re range	Disturber	Disturber Position, ℓ, in.
1	2 inch	12,000 - 100,000	None	—
2	2 inch	11,000 - 23,000	1/4 in.Nozzle	0, 1/2, 1,3, 5, 7, 12
3	2 inch	12,000 - 70,000	1/2 in.Nozzle	0, 1/2, 1,3, 5, 7, 12
4	2 inch	11,000 - 23,000	1/4 in.Orifice	0, 1/2, 1, 3,5, 7, 12
5	2 inch	12,000 - 70,000	1/2 in.Orifice	0, 1/2, 1, 3,5, 7, 12
6	1 inch	14,000 - 100,000	None	—
7	1 inch	14,000 - 70,000	1/2 in.Nozzle	1, 2, 3, 5, 7

over the heat transfer area. The equation used was

$$q = h A_w (T_w - T_a) \tag{31}$$

The heat transferred, q, was calculated from the current passing through and the voltage drop across the resistance wire.

An example of the original data sheet is given in Table (2). All the quantities required in the calculations are noted in it. A sample calculation is shown in appendix 3.

Procedure

In making a run the following procedure was followed:

(a) Cracked ice was placed in the thermos flask and the cold junction of the system immersed in it.

(b) Cold water was supplied to the coolers.

(c) The bypass valve was completely opened and the valve to the test section closed.

(d) The blower was started and the required flow rate through the test section was obtained by adjusting the valve controlling the flow to the test section.

(e) The temperature recorder was adjusted to zero.

(f) After about five minutes the temperature of the incoming air was recorded. The barometric pressure was recorded.

TABLE 2

SAMPLE DATA SHEET

2 inch Test Section. 1/2 inch Nozzle. Group 3

No.	ΔH	T_a	T_{w1}	T_{w2}	T_{w3}	T_{w4}	P_o	P_e	I	V
1	1.18	75.2	129.6	130.6	129.9	129.6	17.5	14.7	0.246	55.3
2	2.23	73.7	128.1	129.6	128.3	128.5	17.5	14.7	0.276	62.8
3	4.19	70.4	128.7	129.6	129.2	128.5	17.5	14.7	0.310	71.0
4	7.07	67.6	127.5	129.7	128.6	128.7	17.3	14.7	0.349	80.0
5	11.0	65.2	129.5	130.5	129.6	129.4	17.3	14.7	0.382	88.0
6	18.8	63.1	127.7	129.5	129.2	128.5	18.0	14.7	0.425	98.0
7	28.0	61.5	127.9	129.5	128.9	128.5	19.9	14.7	0.458	105.5
8	1.20	74.5	128.5	129.1	128.5	128.3	17.6	14.8	0.267	60.6
9	2.37	71.8	129.9	130.9	130.3	130.5	17.4	14.8	0.306	69.9
10	4.14	69.6	128.8	130.0	129.0	129.8	17.4	14.8	0.337	77.1
11	7.02	67.6	128.7	129.8	130.2	129.8	17.2	14.8	0.380	85.0
12	11.1	65.5	130.0	130.7	130.2	130.8	17.2	14.8	0.409	94.8
13	18.5	63.1	--	128.7	128.6	129.0	18.1	14.8	0.439	101.0
14	27.6	61.5	--	129.8	130.1	130.4	20.0	14.8	0.479	111.0
15	1.10	75.0	128.8	129.5	128.4	128.7	17.5	14.7	0.268	60.8
16	2.22	73.0	129.7	130.8	129.5	130.2	17.3	14.7	0.300	68.8
17	4.15	70.0	129.5	130.5	130.0	130.2	17.3	14.7	0.333	76.6
18	6.52	68.9	128.6	129.7	129.3	129.6	17.3	14.7	0.367	83.6
19	10.9	65.4	126.0	128.5	129.1	128.5	17.3	14.7	0.399	91.0
20	18.5	62.1	126.5	128.3	128.6	128.6	18.0	14.7	0.439	100.8
21	27.9	61.0	127.2	128.5	128.5	129.5	19.9	14.7	0.473	109.0

(g) The current through the wire around the test section was started. It was adjusted by the variable transformer to get a temperature of 125-130° F in the test section.

(h) When the temperature in the test section had been steady for five minutes, the e.m.f. readings from all the thermocouples was recorded.

(i) The ammeter and voltmeter readings were noted.

(j) The current through the resistance wire was shut off.

(k) The manometer and the pressure gauge readings were recorded.

(l) The flow through the apparatus was adjusted to a new valve and the procedure from (e) to (k) was repeated for this new flow rate.

(m) After all the data for all the flow rates required had been taken the valve to the test section was closed and the by-pass valve opened.

(n) The blower was shut off.

About 20 minutes to half an hour were required for steady state conditions to be attained at each flow rate.

CHAPTER V

CALCULATION OF DATA

The heat transfer coefficient was calculated by a simple heat balance over the heated copper section. Under steady state conditions all the heat generated in the resistance wire is removed by the air flowing through the pipe assuming no heat loss to the lucite pipe or through the vermiculite insulation. Assuming a constant temperature, T_W, of the copper pipe wall, the average heat transfer coefficient is obtained by the following expression

$$q = hA_W \ (T_W - T_a) \tag{31}$$

The heat input, q, was calculated by measuring the current through the resistance wire and the voltage drop across it. The temperature, T_W, was measured by thermocouples embedded at various positions in the copper as shown in (Figure 3). It was found that the maximum variation in the temperature read from the four thermocouples was 2° F. The wall temperature, T_W, was taken as the average of these four thermocouple readings. The rise in temperature of the air going through the copper section was insignificant so the bulk temperature, T_a, was taken as the temperature of the incoming air.

The maximum error in measuring the average heat transfer coefficient can be found by differentiating equation

(31). This error is given by

$$dh = \frac{dq}{A_W(T_W - T_a)} + \frac{q\, d(T_W - T_a)}{A_W\,(T_W - T_a)^2} \qquad (32)$$

It is assumed that the error in measuring the area of heat transfer, A_W, is negligible. In most cases $T_W - T_a$ was 60° F. and when q was 50 B.T.U./hour, h was approximately 20 B.T.U./hour square feet° F. The error in measuring q was ± 2% and that in $T_W - T_a$ was about ± 1.5%. Substituting these values in equation (32) the maximum error in h, dh, was found to be about 0.83 B.T.U./hour square feet° F. This is equivalent to an error of about ± 4.5%.

The flow rate was calculated by noting the pressure difference across a sharp edged orifice placed before the entrance section. Ambrose's (1, P. 166) calibration for the orifice manometer was used. Ambrose plotted $k = Q\sqrt{\rho_o/\rho_e}$ against the manometer deflection for the orifices used. In the expression ρ_o is the density of the air at the orifice, ρ_e the density at the test section and Q the flow rate in cubic feet per minute measured at 60° F. and one atmosphere pressure. It was assumed that the pressure at the test section was atmospheric. The pressure at the orifice was read from a pressure gauge and the corresponding dead weight pressure found from the calibration curve given by Ambrose

(1, P. 167). The Reynolds number was calculated from the flow rate, Q, by the expression

$$Re = \frac{DU\rho}{\mu} = \frac{(60)\ (D)\ (\rho 60)}{A_c} \left(\frac{Q}{\mu}\right) = \frac{BQ}{\mu} \qquad (33)$$

where B is a constant.

The manometer calibration curve is such that a maximum error of $\pm$ 4% in reading the manometer deflection gives only a $\pm$ 3% error in the flow rate and hence in the Reynolds number.

A sample calculation is given in appendix 3.

CHAPTER VI

ANALYSIS OF DATA

A summary of the complete experimental program is given in Table (1).

All the data taken for runs without any disturbers were correlated by plotting the Nusselt number against the Reynolds number on log log coordinates. These plots are shown in Figure (6) for the 2 inch long section and Figure (7) for the 1 inch section. Also plotted for purposes of comparison are the analytical results of Latzko (8), Deissler (3) and Sleicher and Tribus (13) and the experimental results of Boelter, Young and Iverson (2).

Latzko's equations are for a Prandtl number of unity and the results obtained from his equation (18) for fully developed turbulent flow and uniform wall temperature have been multiplied by the factor $\left(\frac{0.73}{1.00}\right)^{0.3}$. This makes the results valid for the air used in the present investigation. Deissler (3) plots his equations giving the local Nusselt number for various Reynolds numbers. From these the average Nusselt number is found by graphical integration. The average Nusselt number is also calculated by graphical integration from Sleicher and Tribus's equation (20). Sleicher and Tribus suggest that with only the first three eigenvalues

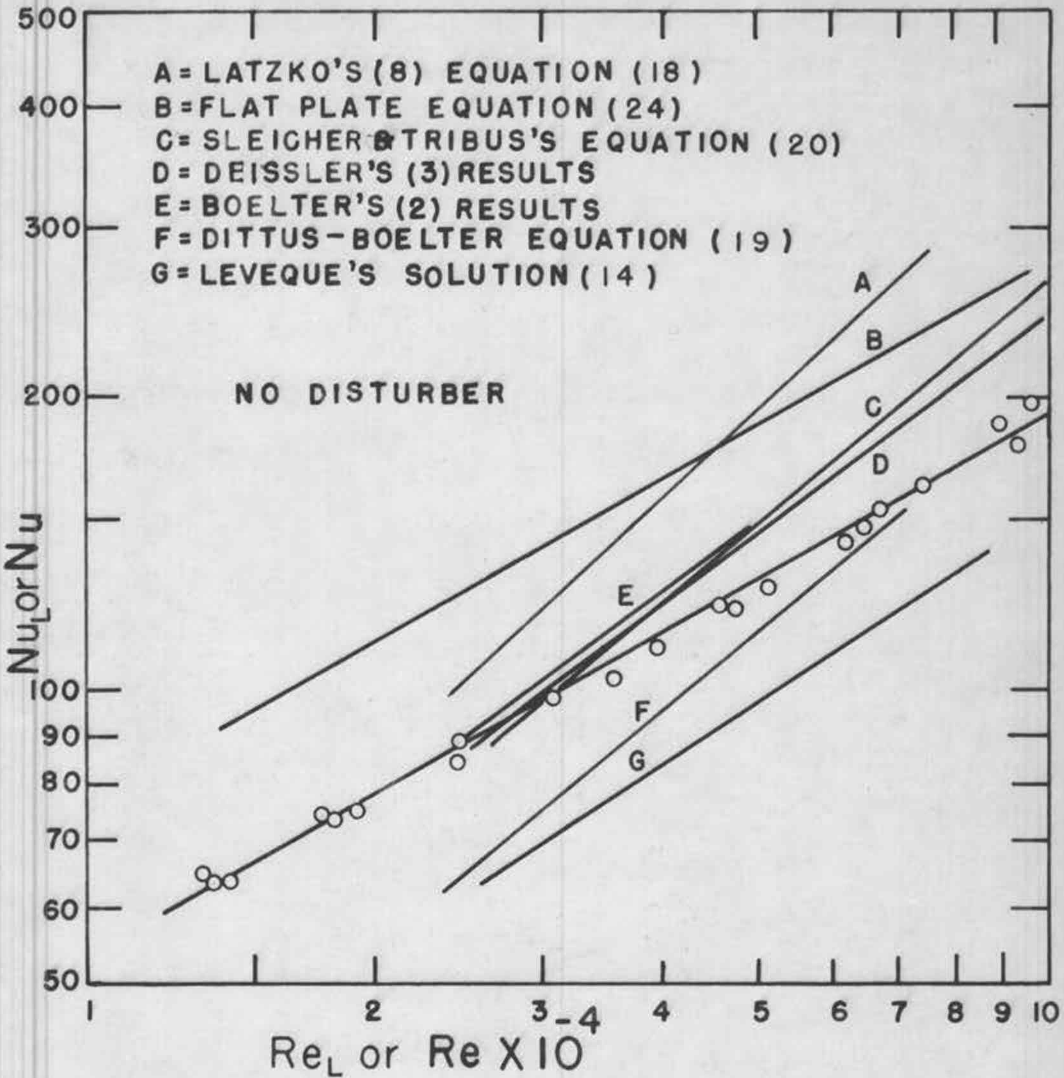

CORRELATION OF DATA

2 INCH SECTION

FIGURE 6

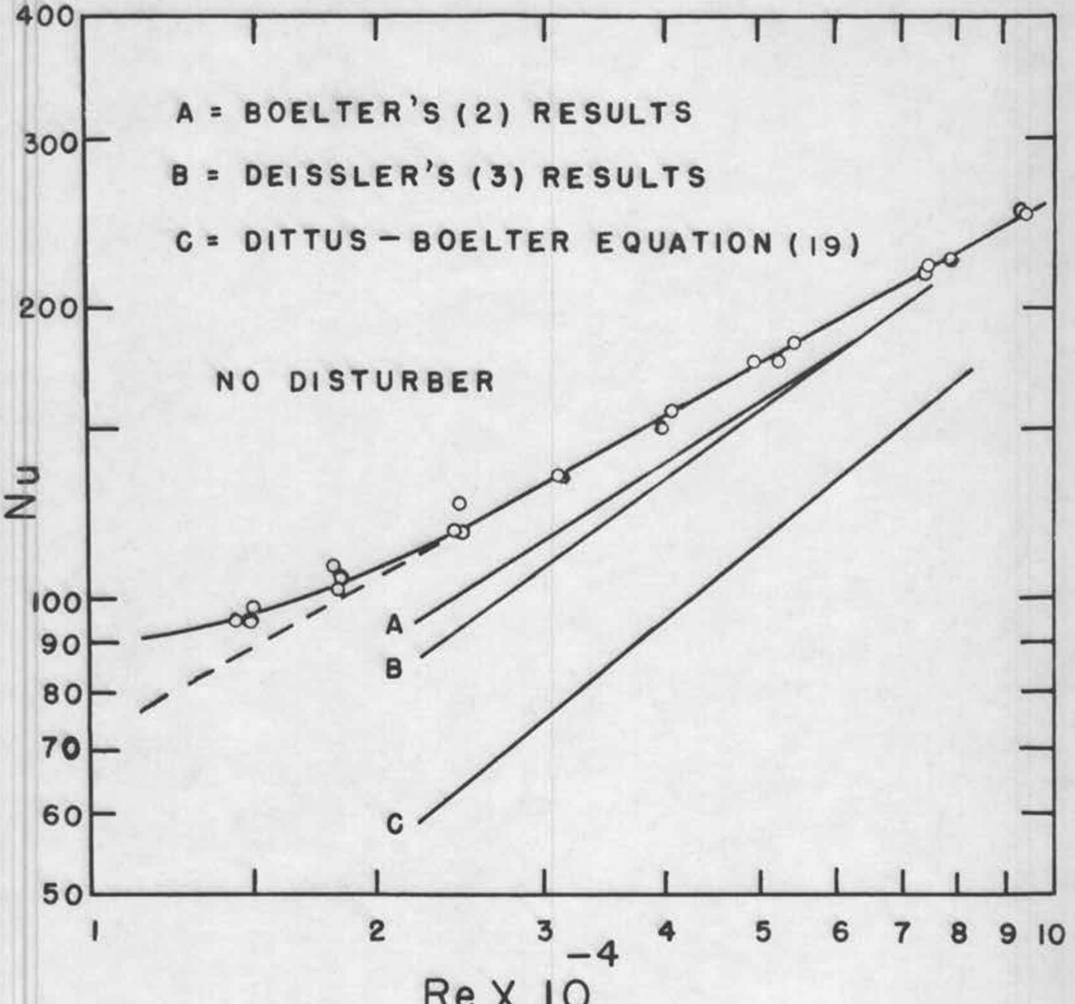

CORRELATION OF DATA

1 INCH SECTION

FIGURE 7

and constants which they give, their equation should be used only for L/D > about 4. Boelter, Young and Iverson (2) give their results for the required conditions in graphical form and the Nusselt numbers are obtained from the appropriate figures.

On Figures (6) and (7) the Dittus-Boelter equation for heating (19) is also shown. The equation for heat transfer from flat plates (24) and Leveque's solution of the energy equation (14) are plotted also.

It is seen that for the 2 inch heating section the experimental data fall on a straight line (Figure 6). Enough points were taken to obtain the equation of this line by least square analysis of the data points. The calculations are shown in appendix (3) and the equation obtained was

$$Nu = 0.343 \, (Re)^{0.547} \tag{34}$$

The conditions for this equation are

(a) Reynolds is between 12,000 and 100,000.

(b) $Pr = 0.73$

(c) $L/D = 2.0$

(d) Constant wall temperature and fully developed turbulent flow.

If the Nusselt number is plotted against L/D with Reynolds number as a parameter, the curves obtained will be of the type shown in Figure (8). These curves are similar to those obtained by Deissler (2). The asymptotic value of Nusselt number for each Reynolds number is that predicted by the Dittus-Boelter equation (19). This means that for large values of L/D, the Nusselt number is proportional to $(Re)^{0.8}$. On the other hand the Nusselt number becomes very large for small values of L/D and in the limit the Nusselt number approaches infinity as L/D approaches zero. This is explained by the fact that the temperature gradient at the entrance of the heat transfer section is infinite. This means that for extremely small values of L/D, the Nusselt number should become independent of the Reynolds number. In between these two limits the dependency of the Nusselt number on the Reynolds number increases with increasing L/D and in the limit becomes proportional to $(Re)^{0.8}$ and independent of L/D. This means that the slope of the plot of log Nu against log Re with L/D as parameter should increase with L/D until it becomes constant at 0.8 for large values of L/D.

However this slope should be a function of the Reynolds number itself. From Figure (8) it is evident that for low Reynolds numbers the asymptotic Nusselt number is reached at comparatively large L/D ratios while for high Reynolds numbers the asymptotic value is reached at comparatively low L/D ratios. So when log Nu is plotted against log Re

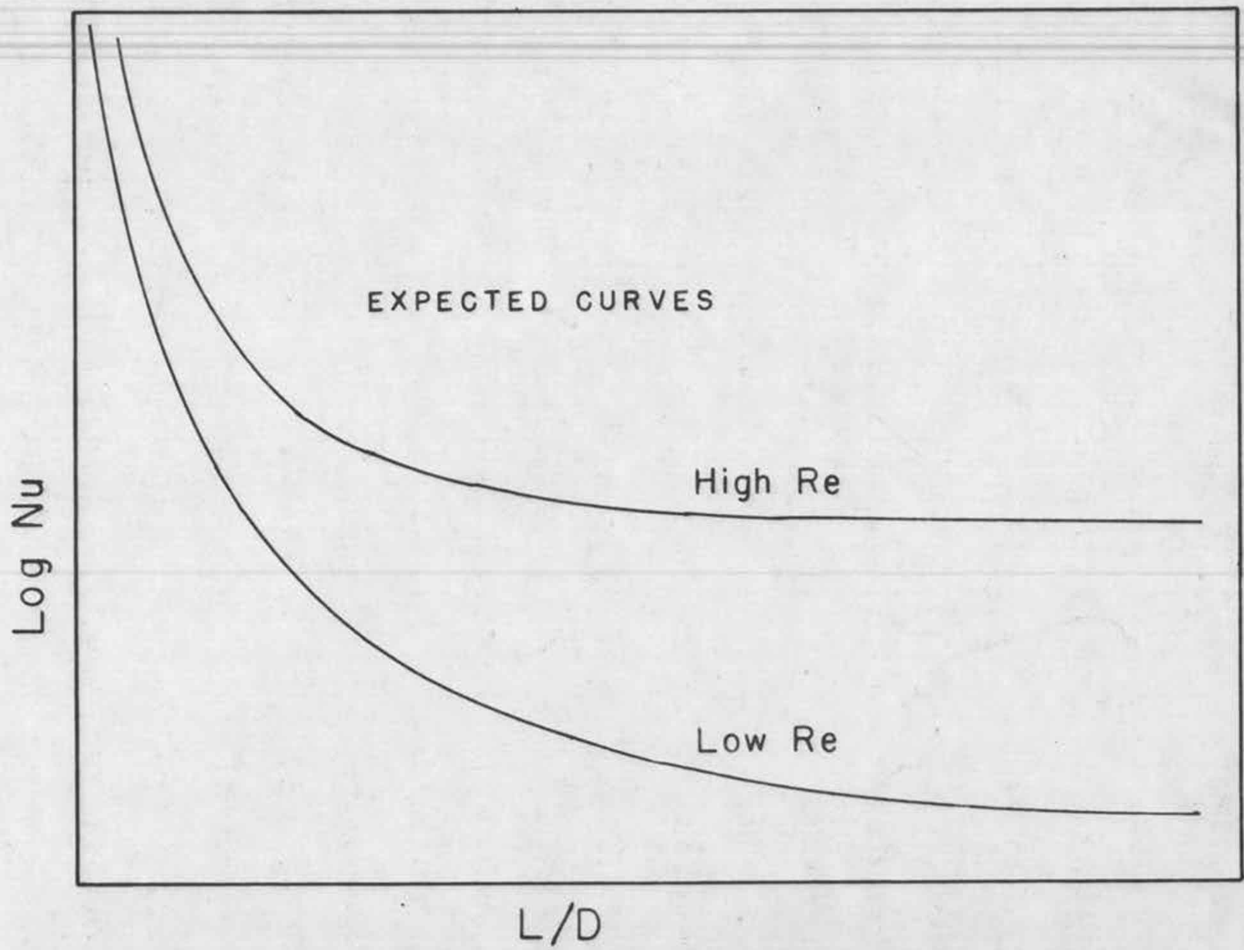

VARIATION OF Nu WITH L/D

FIGURE 8

for a particular L/D value a curve will be obtained such that its slope increases with the Reynolds number until the curve coincides with the Dittus-Boelter equation at large values of Reynolds numbers.

The slope obtained by plotting log Nu against log Re for the 2 inch heating section is 0.547. In this case the variation of the slope with the Reynolds number is discernible only at the lowest Reynolds numbers obtained. Probably the range of Reynolds numbers covered is not large enough to observe an appreciable change in slope. The slope obtained is slightly less than that obtained by plotting the results of various other workers. It is seen that the present results obtained agree with those of the other workers referred to above in the Reynolds number range of 2.5×10^4 to 3.3×10^4. Above this Reynolds number the Nusselt numbers given by the other workers become progressively greater than those obtained in the present experiments.

An interesting comparison of the experimental data with the flat plate energy equation (24) can be made. For heat transfer from a flat plate the Nusselt number is proportional to $(Re)^{0.5}$ while from the experimental data obtained it is seen that for the 2 inch heating section the Nusselt number is proportional to $(Re)^{0.547}$. This suggests that the 2 inch heated section behaves somewhat like a heated flat plate. It is possible that a discontinuity between the copper and the plastic pipe existed because of improper honing. Possibly the copper section diameter even after honing remained slightly smaller than that of the plastic tube. This difference in diameters would introduce a discontinuity in the surface at the junction and a new laminar boundary layer would build up at the upstream end of the heat transfer section. The boundary layer over a flat plate immersed in a flowing fluid forms in the same manner. So it is likely that the Nusselt number would vary with the Reynolds number in the same manner in both cases.

For the 1 inch heating section it is seen that the slope of the plot of log Nu against log Re increases with the Reynolds number (Figure 7). This substantiates the analysis presented above. The equation of the straight line portion of the curve was obtained by least square analysis of the data points. The calculations are shown in appendix (3) and the equation obtained was

$$\mathrm{Nu} = 0.328\,(\mathrm{Re})^{0.580} \tag{35}$$

The conditions for this equation are:

(a) Re between 27,000 and 100,000.

(b) Pr = 0.73.

(c) L/D = 1.0

(d) Constant wall temperature and fully developed turbulent flow.

In Figure (7) the results of two other workers for 1 inch heated sections are also given. For this L/D ratio also the slope obtained is slightly less than that obtained by the other workers. However the difference in slopes is less than the corresponding difference obtained for the 2 inch heated section.

As noted above Deissler's results were integrated graphically to obtain the average Nusselt number. There is an extremely large variation in the local Nusselt numbers in going from $L/D = 0$ to $L/D = 1.0$ and so the integration is not likely to be accurate. So for $L/D = 1.0$ it can be concluded that the average Nusselt numbers obtained from Deissler's results are not accurate. The same can be said for Boelter, Young and Iverson's data. Their first point for calculating the local Nusselt number is at $x/D = 0.5$ and the second is at $x/D = 1.0$. With only two points the curve for the variation of the local Nusselt number with x/D would not be very accurate between $x/D = 0$ and 1.0. Hence the corresponding integration performed by Boelter, Young and Iverson to obtain the average Nusselt number would not be accurate for $L/D = 1.0$. Boelter, Young and Iverson's results show no change in slope between the lines for the 2 inch and the 1 inch heating sections. However according to the analysis given above a change in slope is to be expected. Sleicher and Tribus's equation (20) cannot be used for $L/D = 1.0$ as not enough eigenvalues and constants are given.

The 1 inch heating section was honed very thoroughly to assure that there was not discontinuity at the junction of the copper section and the plastic tube. So in this case the velocity profile in the heated section is certainly that of fully developed turbulent flow and no new boundary layer built at the leading edge of the heating section.

Longwell's (10) numerical method is quite lengthy and involved so the Nusselt number was calculated only for one Reynolds number. For Re = 34,000 the Nusselt number calculated by this method for the 2 inch heating section was 135 and for the 1 inch heating section it was 178. The corresponding values obtained from the present experiments are, respectively, 105 and 139. Longwell's method is based on a knowledge of the total conductivity of heat, $\bar{\varepsilon}_H$, as a function of the radius. Considering that values of $\bar{\varepsilon}_H$ are not known accurately near the pipe wall, the results obtained by Longwell's method are in good agreement with the experimental results. If values of $\bar{\varepsilon}_H$ are known accurately near the wall this method should give fairly accurate results for small L/D ratios.

The effect on the Nusselt number of placing nozzles and orifices at various distances in front of the heated section was also studied. A resumé of the size of the nozzles and orifices studied is given in Table (1). The results are shown in Figures (9, 10, 11, 12) where the Nusselt number is plotted against the Reynolds number for various configurations.

It is seen that in all cases the slope of the lines is the same as the corresponding plot without any disturbers when the distance of the disturber upstream from the copper section was $\geqslant$ 1 inch for the 2 inch heating section and $\geqslant$ 2 inches for the 1 inch heating section. When the disturber was placed flush with the copper section the slope obtained was the highest and it decreased with the distance from the test section becoming constant at the distances given above for the two test sections.

Where both the orifices and the nozzles were used the Nusselt numbers obtained with the orifices were slightly higher than those obtained with the same size nozzles for the same Reynolds numbers. Also for a particular distance away from the heating section the smaller disturber sizes give higher Nusselt numbers than the corresponding larger disturber. The variation of Nusselt number with the distance of the disturber from the test section for a Reynolds number 20,000 is shown in Figure (13). Only those positions where

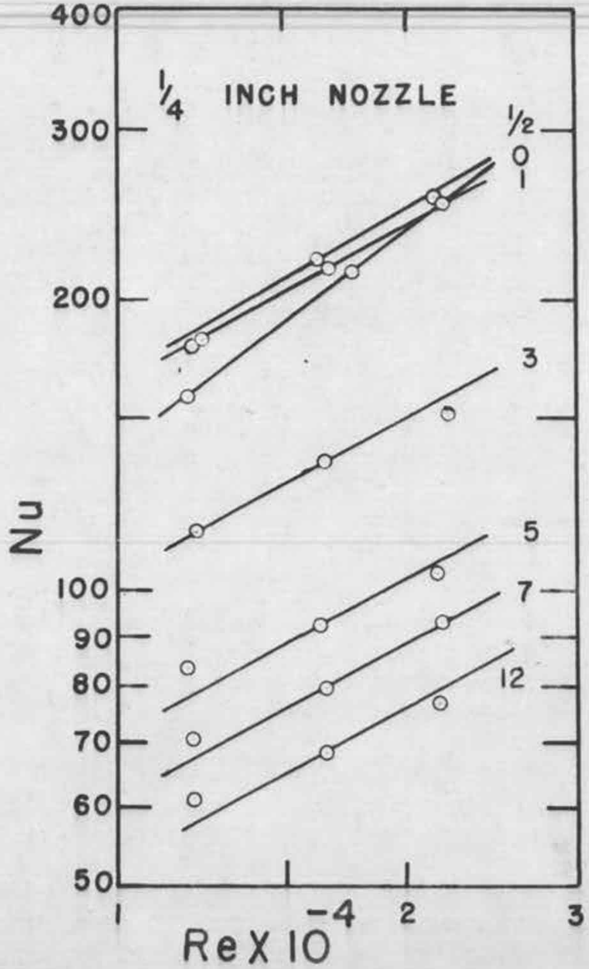

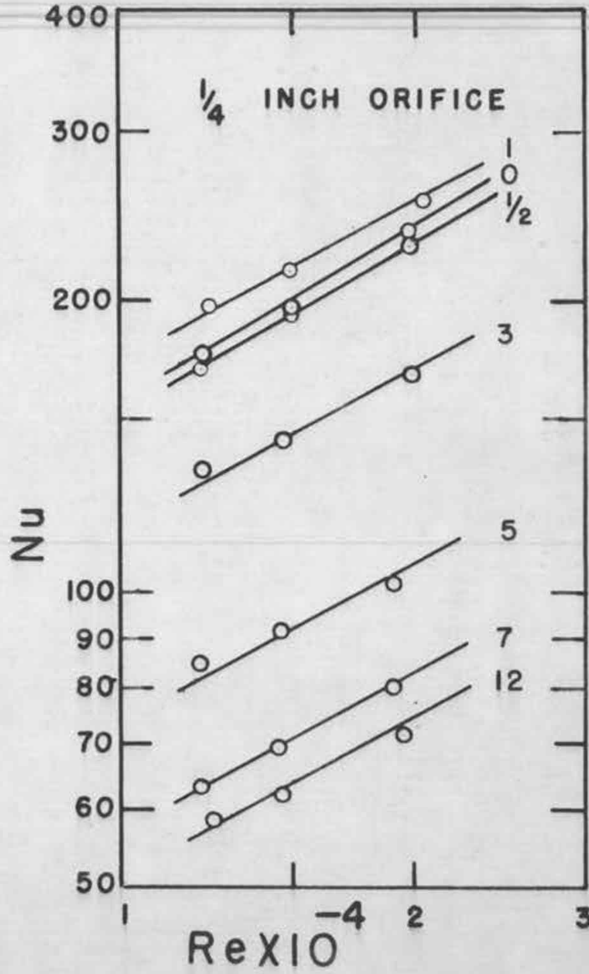

FIGURE 9 CORRELATION OF DATA 2 IN. SECTION

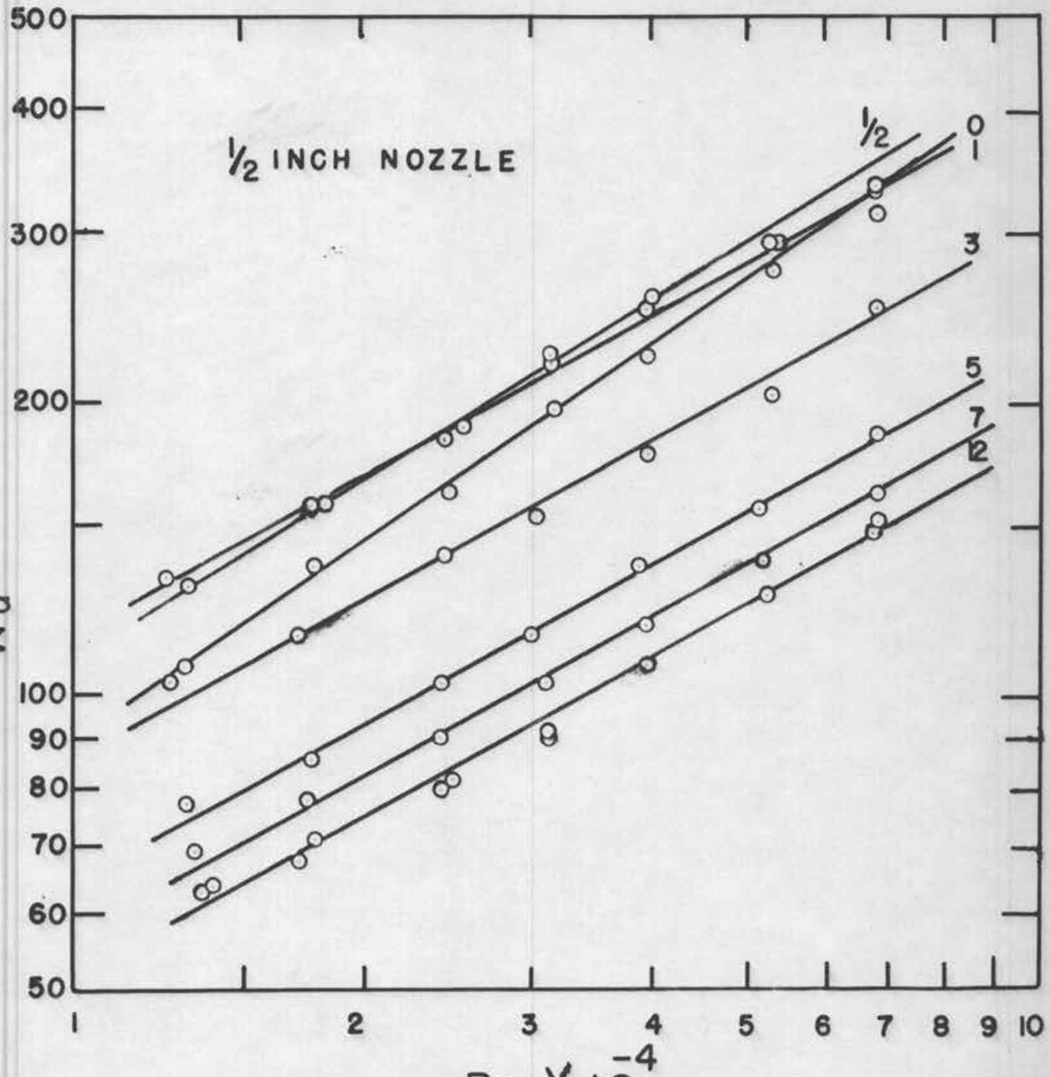

CORRELATION OF DATA

2 INCH SECTION

FIGURE 10

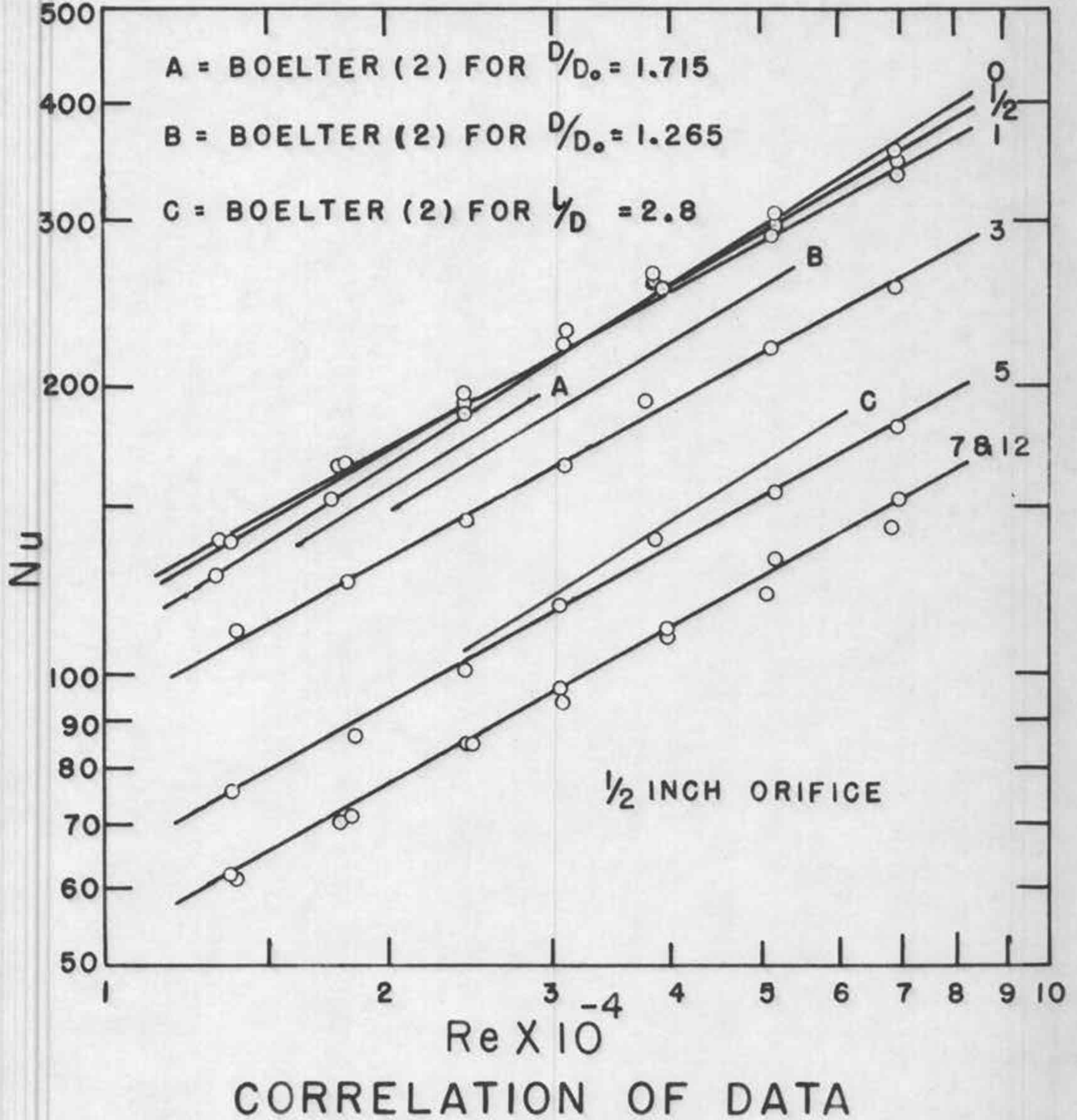

CORRELATION OF DATA
2 INCH SECTION

FIGURE 11

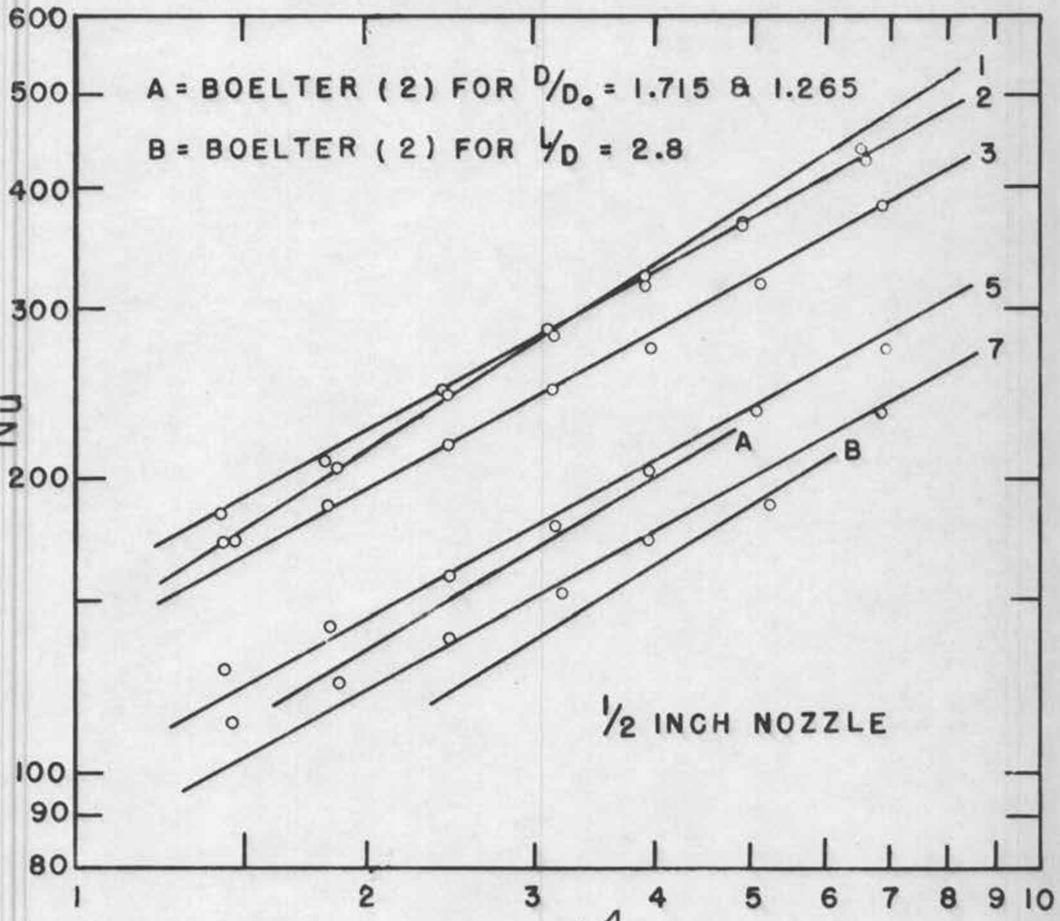

Re X 10^{-4}

CORRELATION OF DATA

1 INCH SECTION

FIGURE 12

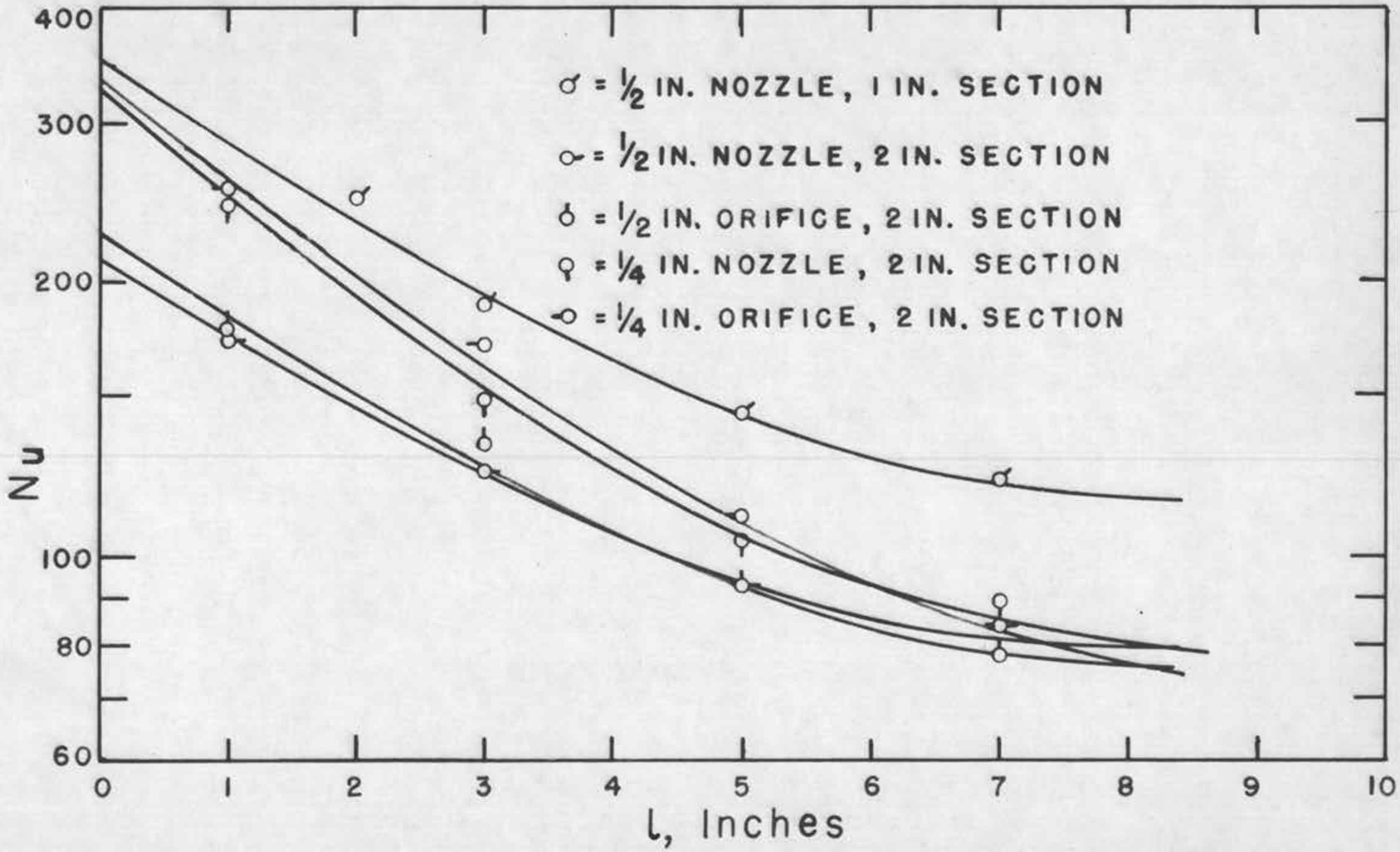

FIGURE 13 VARIATION OF Nu WITH l FOR Re = 20,000

the slope of the line is the same as that obtained without the disturber are considered. It is seen that for the 12 inch position the disturber has no effect on the Nusselt number. At some distance, ℓ_c, between 7 and 12 inches the effect of the disturber becomes negligible and placing it at a distance greater than this does not have any effect on the Nusselt number.

The curves shown in Figure (13) can be represented as a straight line having an equation of the following form

$$\frac{1}{Nu_o - Nu} = \frac{g}{\ell} + b \qquad (36)$$

where Nu_o is the value of the Nusselt number obtained by extrapolating the curves in Figure (13) to $\ell = 0$. The constants g and b were determined by plotting $\frac{1}{Nu_o - Nu}$ against $\frac{1}{\ell}$. Table (3) shows the values obtained for these constants and for Nu_o. The straight lines obtained are shown in Figure (14). The equations obtained are valid only for values of ℓ between 1 inch and ℓ_c for the 2 inch heating section and 2 inch and ℓ_c for the 1 inch heating section. The plot of the equation between these regions is shown by a solid line in Figure (14).

For purposes of comparison Boelter, Young and Iverson's results for the following entrance conditions are also shown in Figures (11, 12).

TABLE 3

Constants for Equation (36) at Re = 20,000

Test Section	Disturber	Nu_o	$g \times 10^3$	$b \times 10^3$
2 inch	1/4 in. nozzle	322	9.7	2.7
2 inch	1/2 in. nozzle	210	21.8	4.8
2 inch	1/4 in. orifice	333	9.7	2.7
2 inch	1/2 in. orifice	222	17.7	4.6
1 inch	1/2 in. nozzle	351	10.0	2.9

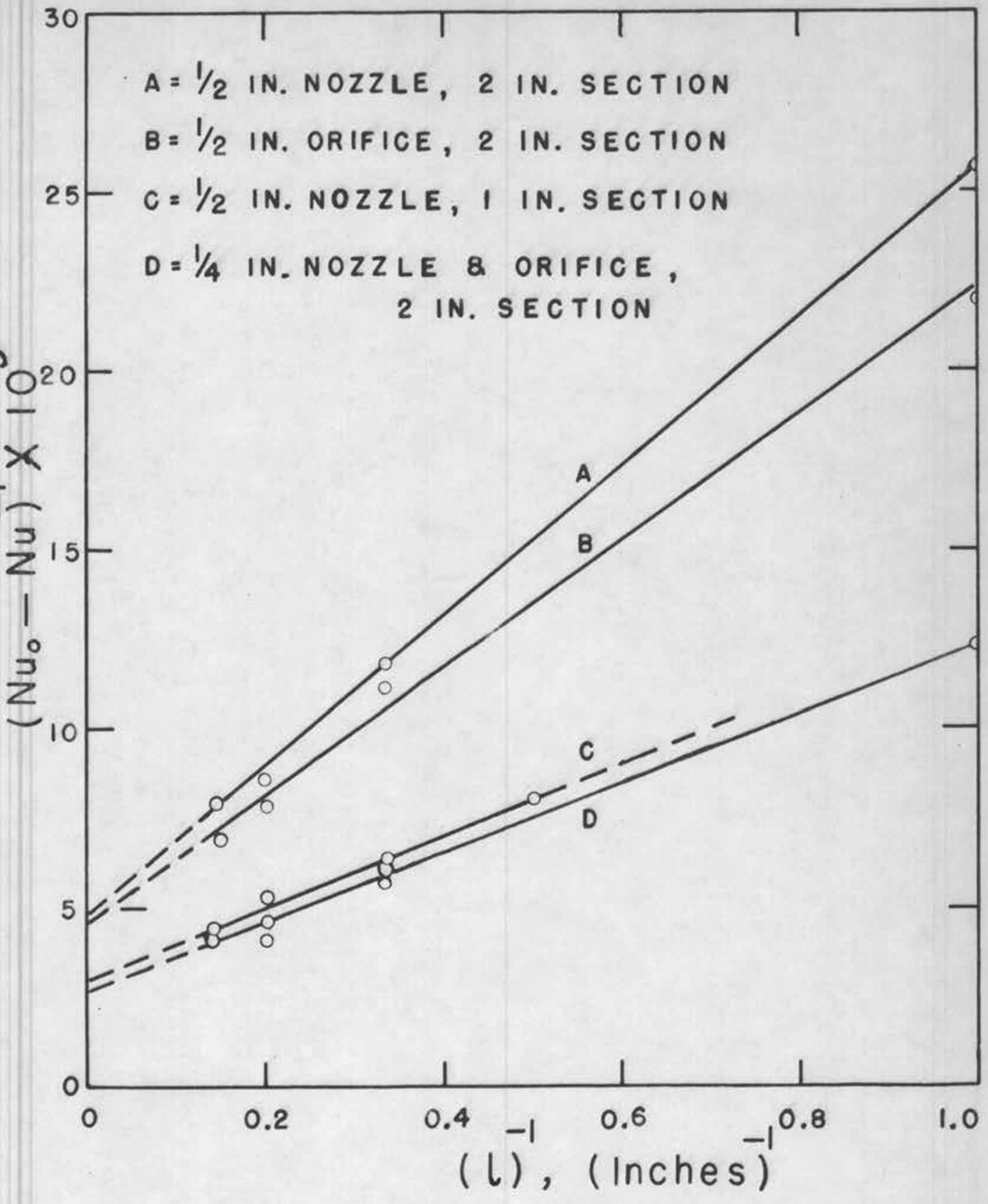

PLOT OF $(Nu_o - Nu)^{-1}$ VS $(l)^{-1}$

FOR Re = 20,000

FIGURE 14

(a) Short calming section $l/D = 2.8$

(b) Large orifice at entrance $D/D_o = 1.265$

(c) Small orifice at entrance $D/D_o = 1.715$

It is not known whether the orifices were placed flush with the heating section or a few inches away from it. However, probably both were placed the same distance away from the entrance to the heating section. These D/D_o ratios are less than those used in the present experiments. It is seen that for both 2 inch and 1 inch heating sections at any fixed Reynolds number there is very little difference in the Nusselt number obtained with either of the orifices used in the above reference.

Boelter, Young and Iverson's results show that for both orifices the Nusselt number for one Reynolds number increased with L/D reaching a maximum and then decreased for any further increase in L/D. For the large orifice this maximum was reached at L/D of about 2 and for the small one at L/D of about 4. The authors explained this by saying that a small region exists immediately downstream of the orifice in which the fluid adjacent to the wall is stagnant.

No such results are obtained for the 1/2 inch nozzle which has been tested with both the 2 inch and the 1 inch heating sections. It is seen that the Nusselt number obtained with L/D = 1 is always greater than that obtained with L/D = 2 for the 1/2 inch nozzle placed at equal distances away from the heating section.

The increase in the Nusselt number obtained by placing a disturber in front of the heated section can be explained by the resulting flow pattern. The disturber provides a sudden expansion and causes considerable turbulence in the emerging air. This gives rise to eddies in the region adjacent to the pipe wall. At a short distance downstream of the disturber the eddies die out and a laminar boundary layer starts building up and about 8 - 10 diameters downstream the flow becomes essentially fully developed turbulent flow. This distance is the distance ℓ_c mentioned above.

The presence of eddies considerably increases the amount of heat transferred. When the test section is immediately downstream from the disturber the heat transfer takes place in the presence of eddies and hence a high Nusselt number is obtained. As the disturber is moved further from the test section, there would no longer be extreme turbulence at the test section and a laminar boundary layer would be forming. Both these phenomena contribute to the decrease in the Nusselt number as ℓ increases.

CHAPTER VII

CONCLUSIONS

As only two different length of heated section to pipe diameter ratios were studied no empirical expression for the effect of this ratio on the average Nusselt can be given. However for L/D = 2 the experimental data obtained could be related by the expression

$$Nu = 0.343 (Re)^{0.547} \tag{34}$$

This relationship holds over the Reynolds number range $12,000 < Re < 100,000$. Below this range a plot of log Nu versus log Re appears to become curved, i.e. the slope of the line is also a function of the Reynolds number.

As pointed out in the previous chapter there is a possibility that a discontinuity existed at the junction between the copper section and the lucite pipe. On the other hand the data obtained is very consistent in itself and studies of more L/D ratios are needed for a more complete understanding of the problem.

The slope of the line obtained from the above equation by plotting log Nu versus log Re is slightly less than the corresponding slope obtained for the 1 inch heated section. According to the analysis presented in the previous chapter the slope should increase with L/D ratios reaching a maximum of 0.8. This difference however is small. Large differences in slope may not be detected until very short sections are encountered.

For the 1 inch heating section the plot of log Nu versus log Re is curved up to a Reynolds number of 27,000. Beyond this point the line is straight and can be expressed by the relation

$$Nu = 0.328 \, (Re)^{0.580} \tag{35}$$

This relationship holds over the Reynolds number range $27{,}000 < Re < 100{,}000$. The change in slope of the plot of log Nu versus log Re as Reynolds number changes is as expected and was detected only slightly for the L/D ratio of 2. For the L/D = 1 case the section was honed very thoroughly and it is certain that no discontinuities existed at the junction of the copper section and the lucite pipe.

The data thus obtained from this work can be used to predict values of the Nusselt number for any Reynolds number within the range of Re = 12,000 to Re = 100,000 for L/D ratios of 1 and 2 and for Pr = 0.73. Further work is needed to determine the effect of L/D ratios.

The effect of placing nozzles or orifices in front of the test section can be predicted by an expression of the form

$$\frac{1}{Nu_o - Nu} = \frac{g}{\ell} + b \qquad (36)$$

where Nu_o, g and b are constants obtained as explained in the previous chapter. Values of these constants obtained for the various entrance configurations and test sections studied are given in Table (3). An expression of this type can be obtained for any Reynolds number required.

CHAPTER VIII

RECOMMENDATIONS

In conducting this study several interesting facts have been noted and investigations along these lines are proposed:

(a) One of the main objects of the present investigation was to study the effect of the ratio of the heated section length to pipe diameter on the heat transfer coefficient. Along these lines two ratios were studied. It is recommended that more ratios be studied with particular emphasis being laid on ratios less than one. For these small ratios the data available is not adequate.

(b) Another line of investigations proposed is the study of the effect of various other types and sizes of entrance configurations on the heat transfer coefficient.

(c) In the present study only one fluid, air, was used. A similar study employing various other fluids would yield information on the effect of the Prandtl number on the heat transfer coefficient.

(d) It has been noted previously that Longwell's (10) graphical method would give reliable results. However his method is very lengthy. A study on programming of a computer for solving the energy equation by Longwell's method could be made. Use of a computer would save a considerable amount of time in using Longwell's method.

CHAPTER IX

NOMENCLATURE

The fundamental dimensions are represented by the following letters:

F : Force

L : Length

m : mass

t : time

T : Temperature

Symbol	Meaning	Dimensions
a	Thermal diffusivity, $\frac{k}{C_p \rho}$	L^2/t
A_c	Area of cross-section of the tube	L^2
A_w	Area of surface over which heat transfer takes place	L^2
A_n	Constants used in Equation (20)	None
b	Constant used in Equation (36)	Variable
C	Velocity gradient	t^{-1}
C_p	Specific heat of the fluid at constant pressure	FL/mT
D	Inside diameter of pipe	L
D_o	Nozzle or Orifice Diameter	L
f	Friction factor	None

f_1, f_2 f_3	Function	---
g	Constant used in Equation (36)	None
h	Average heat transfer coefficient	F/LtT
h_l	Local heat transfer coefficient	F/LtT
ΔH	Deflection of orifice manometer	L
I	Current supplied to resistance wire	Amperes
k	Thermal conductivity of the fluid	F/tT
ℓ	Distance of disturber from entrance to test section	L
L	Total length of test section	L
q	Heat supplied to test section	FL/t
Q	Air flow rate, cubic feet per minute measured at 60° F. and 1 atmosphere pressure	L^3/t
r	Radial distance measured from the center of a pipe	L
r_w	Radial distance to the pipe wall measured from the center of a pipe	L
t	Time	t
T	Temperature of the fluid	T
T_a	Bulk temperature of the entering fluid	T
T_w	Temperature of the surface from which heat transfer takes place	T
T	Temperature of the undisturbed stream	T
u	Velocity of the fluid in the x direction	L/t

u^+	Dimensionless velocity parameter	None
U	Average velocity of undisturbed flowing stream; average velocity in a pipe	L/t
v	Velocity of the fluid in the y direction	L/t
V	Voltage drop across the resistance wire	Volts
w	New variable introduced in the graphical solution of Equation (10), the energy equation, $\int_{r_w}^{r} \frac{d(r_w - r)}{r\bar{\varepsilon}_H}$	t/L^2
x	Cartesian coordinate; distance from the point of beginning heat transfer	L
y	Cartesian coordinate; distance measured normal to the solid boundary	L
α	Ratio of the eddy diffusivity of heat, ε_H, to the eddy diffusivity of momentum, ε_M	None
δ	Thickness of hydrodynamical boundary layer	L
ε_H	Eddy diffusivity of heat	L^2/t
$\bar{\varepsilon}_H$	Total diffusivity of heat	L^2/t
ε_M	Eddy diffusivity of momentum	L^2/t
λ_n	Eigenvalues	---
μ	Viscosity of the fluid	m/Lt
ρ	Density of the fluid	m/L^3
ϕ	Dimensionless temperature, $(T_w - T)/(T_w - T_a)$	None

Dimensionless Groups:

Nu	Average Nusselt number, $\frac{hD}{k}$
Nu_1	Local Nusselt number, $\frac{h_1 D}{k}$
Nu_L	Total Nusselt number for flow over flat plates, $\frac{hL}{k}$
Nu_x	Local Nusselt number for flow over flat plates, $\frac{h_1 x}{k}$
Pr	Prandtl number, $\frac{C_p \mu}{k}$
Re	Reynolds number, $\frac{DU\rho}{\mu}$
Re_x	Local Reynolds number for flow over flat plates, $\frac{xU\rho}{\mu}$
Re_L	Total Reynolds number for flow over flat plates, $\frac{LU\rho}{\mu}$

BIBLIOGRAPHY

1. Ambrose, Tommy W. Local shell-side heat transfer coefficients in baffled tubalar exchangers. Ph.D. thesis. Corvallis, Oregon State College, 1957. 183 numb. leaves.

2. Boelter, L. M. K., G. Young and H. W. Iverson. An investigation of aircraft heaters. XXVII.--Distribution of heat-transfer rate in the entrance section of a circular tube. Washington, 1948. 53 p. (U. S. National Advisory Committee for Aeronautics. Technical Note no. 1451)

3. Deissler, Robert G. Analysis of turbulent heat transfer and flow in the entrance regions of smooth passages. Washington, 1953. 80 p. (U. S. National Advisory Committee for Aeronautics. Technical Note no. 3016)

4. Eckert, E. R. G. Introduction to the transfer of heat and mass. New York, McGraw-Hill. 1950. 284 p.

5. Jakob, Max. Heat transfer. Vol. 1. New York, John Wiley, 1950. 758 p.

6. Jenkins, R. Variation of the eddy conductivity with Prandtl modulus and its use in prediction of turbulent heat transfer coefficients. (Heat Transfer and Fluid Mechanics Institute, Stanford University, Stanford, California. Preprints of Papers, June, 1951, p. 147-158)

7. Knudsen, James G. and Donald L. Katz. Fluid dynamics and heat transmission. New York, McGraw-Hill, 1958. 576 p.

8. Latzko, H. Heat transfer in a turbulent liquid or gas stream. Washington, 1944. 58 p. (U. S. National Advisory Committee for Aeronautics. Technical Memorandum no. 1068)

9. Leeds and Northrup Company. Standard conversion tables for Leeds and Northrup thermocouples. Philadelphia, n.d., 43 p.

10. Longwell, P. A. Graphical solution of turbulent flow diffusion equations. American Institute of Chemical Engineers Journal 3:353-360. 1957.

11. Sellars, J. R., Myron Tribus and J. S. Klein. Heat transfer to laminar flow in a round tube or a flat conduit.--The Graetz problem extended. Transactions of the American Society of Mechanical Engineers 78:441-448. 1956.

12. Sleicher, C. A., Jr. Experimental velocity and temperature profiles for air in turbulent pipe flow. Transactions of the American Society of Mechanical Engineers 80:693-704. 1958.

13. Sleicher, C. A., Jr. and M. Tribus. Heat transfer in a pipe with turbulent flow and arbitrary wall-temperature distribution. (Heat Transfer and Fluid Mechanics Institute, Stanford University, Stanford, California. Preprints of Papers, June, 1956, p. 59-78.

APPENDIXES

APPENDIX I

CALCULATION OF THE NUSSELT NUMBER FROM OTHER WORKERS DATA AND EQUATIONS

LONGWELL'S GRAPHICAL METHOD

To calculate the Nusselt number by the numerical method developed by Longwell the outline given in his article (10) was followed. The Nusselt number was calculated for a Reynolds number of 34,000.

First the velocity profile in the pipe was calculated. The following equations were used to calculate the point velocities:

$$u^+ = y^+ \quad \text{for} \quad y^+ < 5$$

$$u^+ = 5.0 \ \ln y^+ - 3.05 \qquad 5 < y^+ < 30$$

$$u^+ = 2.5 \ \ln y^+ + 5.5 \qquad y^+ > 30$$

where $u = \dfrac{u}{U\sqrt{f/2}}$ and $y^+ = \dfrac{y}{r_w} \dfrac{Re}{2} \sqrt{\dfrac{f}{2}}$

In these expressions u is the point velocity and U the average velocity.

The following expressions were used to calculate the total diffusivity of heat, $\bar{\varepsilon}_H$:

$$\bar{\varepsilon}_H = \varepsilon_H + a$$

$$\varepsilon_H = \alpha \varepsilon_m$$

Values of α were taken from Sleicher (13). At the Reynolds number used

$$\alpha = 1.4 \quad \text{for} \quad y^+ < 40$$

$$\alpha = 1.3 \quad \text{for} \quad 40 < y^+ < 100$$

$$\alpha = 1.8 \quad \text{for} \quad y^+ > 100$$

The eddy diffusivity of momentum, $\mathcal{E}_m$, was calculated from the equation given by Knudsen and Katz (7, p. 437).

$$\left(\frac{\mu}{\rho}\right)\mathcal{E}_m = \frac{1 - y^+/R}{du^+/dy^+} - 1$$

where $R = \frac{Re}{2}\sqrt{\frac{f}{2}}$

The derivatives were found from the velocity profile equations given above. However this equation gave a value of $\mathcal{E}_m$ and hence $\mathcal{E}_H$ equal to zero at the center of the pipe. It is known that the eddy diffusivity at the center is not zero so the total diffusivity was extrapolated near the center of the pipe. This extrapolation is shown by a dotted line in Figure (15) where the total diffusivity of heat is plotted against the radius.

The function f_3 (w) was calculated by use of the expression $f_3(w) = \frac{1}{ur^2 \bar{\mathcal{E}}_H}$. The new variable, w, was found by graphical integration of the equation $dw = \frac{d(r_w - r)}{r\,\bar{\mathcal{E}}_H}$.

The results are tabulated in Table (4). In this Table the point velocities and the total diffusivities are also given.

To obtain the appropriate intervals in w to be used in the final graphical solution the function f_3 (w) was plotted against the variable w (Figure (16)). At the minimum in this curve it can be assumed that $\Delta w_{n+1} = \Delta w_{n-1}$ so equation (30) becomes

$$(\Delta w_{n-1})^2 = 2\,(\Delta x)\, f_3\,(w_n) \tag{37}$$

A value of Δx is assumed and the initial interval, Δw_{n-1}, is calculated from equation (37). The successive intervals towards the wall are then calculated by the use of equation (30) and the plot of $f_3\,(w)$ against w. If the final value of w calculated coincides with the wall a correct value of Δx has been assumed. If not another value of Δx is assumed and with the help of equations (30 and 37) and Figure (16) the whole process is repeated until the final value of w obtained coincides with the wall.

After a few tries it was found that by assuming $\Delta x = 0.1$ inch the last value of w calculated coincided with the wall. The calculations for $\Delta x = 0.1$ inch are shown in Table (5).

A Schmidt type construction was then made with ϕ as ordinate and w as abscissa. The values of w used were calculated as above. A Schmidt-type construction makes use of the approximation

$$\phi_{(m+1,\,n)} = \frac{1}{2(\Delta w_n)} \Big[(\phi_{m,\,n-1})\,(\Delta w_{n-1}) + (\phi_{m,\,n+1})\,(\Delta w_{n+1}) \Big]$$

where the subscript n refers to the variable x and n to w.

The construction is shown in Figure (17). For the sake of clarity only a few of the steps are shown.

The values of r corresponding to the values of w used in the Schmidt plot were found by the help of Figure (16) and the definition of f_3 (w). The temperature profiles were drawn for various values of Δx. These are shown in Figure (18). In this figure the dimensionless temperature ϕ is plotted against the radius. The local Nusselt number is given by

$$Nu_l = - \frac{D}{T_w - T_a} \left(\frac{\partial \phi}{\partial y} \right)_{y = o}$$

The local Nusselt number was calculated by the above expression at various values of x and the average Nusselt numbers over 1 and 2 inch lengths were found by graphical integration. The local and average values obtained are given below:

$x = 0.3$ inch $\quad Nu_l = 175$

$x = 0.5$ inch $\quad Nu_l = 156$

$x = 1.0$ inch $\quad Nu_l = 118$

$x = 1.5$ inch $\quad Nu_l = 111$

$x = 2.0$ inch $\quad Nu_l = 104$

The average Nusselt number for $L/D = 2.0$ is 135.

The average Nusselt number for $L/D = 1.0$ is 178.

OTHER WORKERS RESULTS

Boelter, Young and Iverson's (2) results for various entrance configurations are given in Table (6). The authors give average values of the heat transfer coefficients. Deissler (3) gives values of the local Nusselt number for heat transfer from various L/D ratios at fixed Reynolds number. The average Nusselt numbers for L/D = 1 and 2 were obtained by graphical integration. The local and average values obtained are given in Table (7). In this table the local and average values of the Nusselt number obtained by use of Sleicher and Tribus's equation (20) are also given.

Use of Latzko's equation (18) gave the following values of the average Nusselt number:

$$Re = 30{,}000 \qquad Nu = 122$$

$$Re = 60{,}000 \qquad Nu = 230$$

Use of Leveque's solution for turbulent flow in a pipe (14) gave the following values of the average Nusselt number:

$$Re = 30{,}000 \qquad Nu = 70.2$$

$$Re = 60{,}000 \qquad Nu = 120$$

It was found that the factor $\left(\frac{f}{18}\right)^{1/3}$ is nearly constant over the range of Reynolds number covered.

TABLE 4

Quantities used in the Graphical Solution

r (inches)	U (ft./sec)	$\bar{\varepsilon}_H \times 10^4$ (sq.ft./sec)	$f_3(w)\ 10^{-2}$ (sec^2/ft^5)	w (sec/sq.ft)
0.4973	--	3.0	--	--
0.4945	300	4.57	42.490	--
0.4918	372	6.53	23.849	39.0
0.4891	424	8.72	16.211	--
0.4864	464	11.08	11.854	--
0.4836	496	13.56	9.406	54.5
0.4782	524	32.4	3.779	--
0.4727	542	40.0	2.973	69.04
0.4672	560	47.4	2.485	--
0.4618	574	54.4	2.163	70.20
0.4563	585	61.8	1.913	--
0.4509	595	68.7	1.732	--
0.4454	605	75.2	1.596	79.48
0.4181	641	97.9	1.314	86.83
0.3908	666	122.0	1.161	93.07
0.3635	686	141.4	1.124	98.55
0.3362	705	157.2	1.149	103.74
0.3089	715	168.3	1.254	108.93
0.2816	729	175.6	1.419	114.39
0.2543	737	178.3	1.696	120.15
0.2270	749	176.8	2.110	126.54
0.1997	756	169.2	2.823	133.86
0.1724	764	161.2	3.934	142.70
0.1451	771	152.2	6.065	153.98
0.1178	728	129.0	10.102	168.96
0.0905	785	105.3	18.811	189.68
0.0632	790	78.2	41.493	220.77
0.0459	794	46.7	83.14	268.90
0.0086	800	11.56	2432.4	445.26

TABLE 5

Values of $f_3(w_n)$ and w_{n-1} Calculated for $\Delta x = 0.1$ inch

$f_3(w_n)$ (Sec^2/ft^5)	Δw_{n-1} (Sec/sq.ft)	w_{n-1} (Sec/sq.ft)	r (inches)
		99.00	
111	1.36	97.64	
112	1.37	96.27	
113	1.37	94.90	
114	1.38	93.52	
116.5	1.40	92.12	
119	1.42	90.70	
121	1.42	89.28	
124	1.45	88.83	
126	1.46	86.87	
131.4	1.50	85.37	
135	1.50	83.85	
140	1.55	82.32	
144.5	1.55	80.77	
150	1.61	79.16	0.4447
159	1.65	78.15	0.4475
165	1.67	76.84	0.4510
173	1.73	75.11	0.4560
187	1.80	73.31	0.4610
209	1.94	71.17	0.4664
237	2.04	69.13	0.4726
290	2.37	66.76	0.4778
382	2.68	64.08	0.4798
500	3.11	60.87	0.4811
620	3.32	57.55	0.4827
785	3.82	53.73	0.4847
1000	4.36	49.37	0.4874
1300	4.97	44.40	0.4893
1660	5.56	38.84	0.4909
2200	6.60	32.24	0.4929
3100	7.83	24.41	0.4950
5200	9.93	14.48	0.4966
8400	14.20	0.28	0.5000

TABLE 6

Summary of Boelter, Young and Iverson's Results

Re	$\frac{L}{D}$	Nu: Long Calming Section $\ell/D = 11.2$	Short Calming Section $\ell/D = 2.8$	Small Orifice $D/D_o = 1.715$	Large Orifice $D/D_o = 1.265$
27,200	2	92	--	--	--
	1	104	--	--	--
36,400	2	117	--	--	--
	1	130	--	--	--
43,000	2	136	--	--	--
	1	149	--	--	--
48,800	2	146	--	--	--
	1	158	--	--	--
53,000	2	153	--	--	--
	1	164	--	--	--
26,700	2	--	113	--	--
	1	--	128	--	--
36,900	2	--	129	--	--
	1	--	152	--	--
42,200	2	--	148	--	--
	1	--	163	--	--
48,400	2	--	165	--	--
	1	--	179	--	--
54,400	2	--	183	--	--
	1	--	201	--	--
17,000	2	--	--	142	--
	1	--	--	117	--
22,900	2	--	--	168	--
	1	--	--	140	--
26,400	2	--	--	188	--
	1	--	--	150	
22,000	2	--	--	--	157
	1	--	--	--	141
30,700	2	--	--	--	193
	1	--	--	--	172
40,100	2	--	--	--	226
	1	--	--	--	197
49,700	2	--	--	--	252
	1	--	--	--	234

TABLE 7

Deissler's and Sleicher and Tribus's Results

Re	$\frac{x}{D}$	Nu_1 Deissler	Nu_1 Sleicher and Tribus	Nu Deissler	Nu Sleicher and Tribus
100,000	2.00	202	237	223 (L/D = 2)	244 (L/D = 2)
	1.75	206	--	253 (L/D = 1)	
	1.50	210	240		
	1.25	215	--		
	1.00	220	248		
	0.75	227	--		
	0.50	242	253		
	0.25	267	--		
	0	--	256		
60,000	2.00	139	159	157 (L/D = 2)	164 (L/D = 2)
	1.75	141	--	175 (L/D = 1)	
	1.50	144	162		
	1.25	147	--		
	1.00	151	165		
	0.75	157	--		
	0.50	168	168		
	0.25	186	--		
	0	--	173		
30,000	2.00	82	93.5	96 (L/D = 2)	97.6 (L/D = 2)
	1.75	83	--	110 (L/D = 1)	
	1.50	85	95.5		
	1.25	87	--		
	1.00	90	98.0		
	0.75	95	--		
	0.50	101	100		
	0.25	149	--		
	0	--	104		

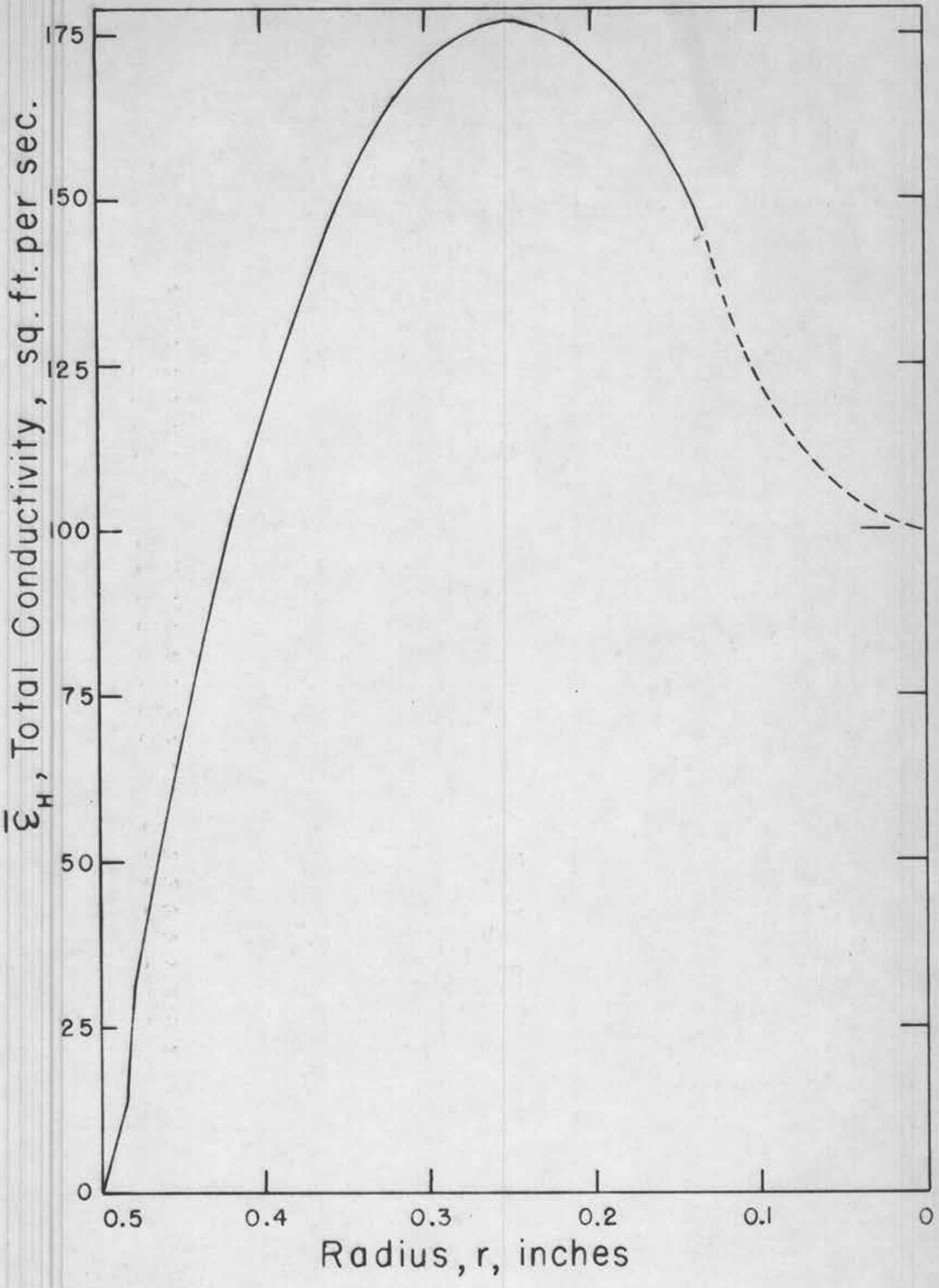

FIGURE 15 TOTAL CONDUCTIVITY

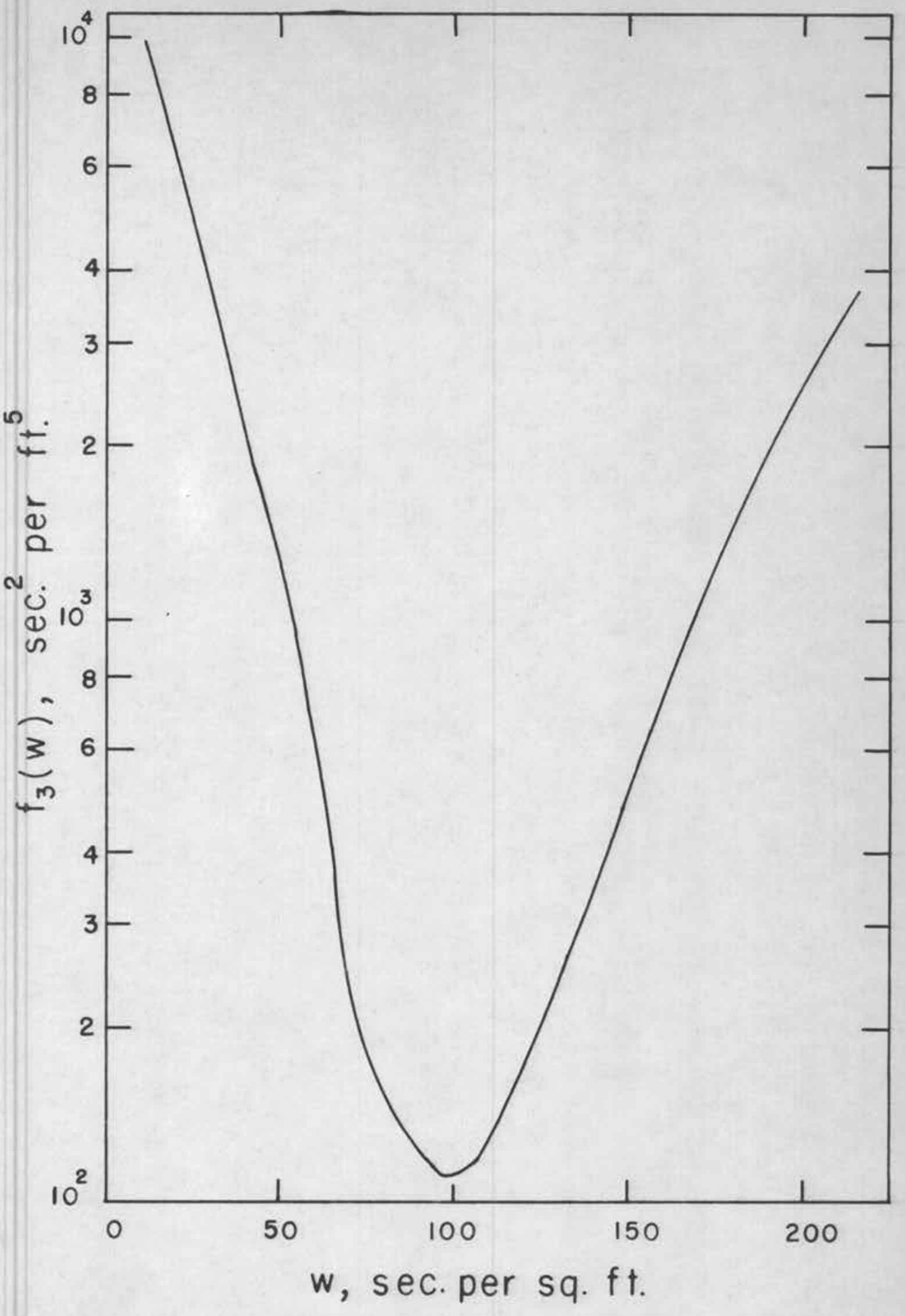

VARIATION OF $f_3(w)$ WITH w

FIGURE 16

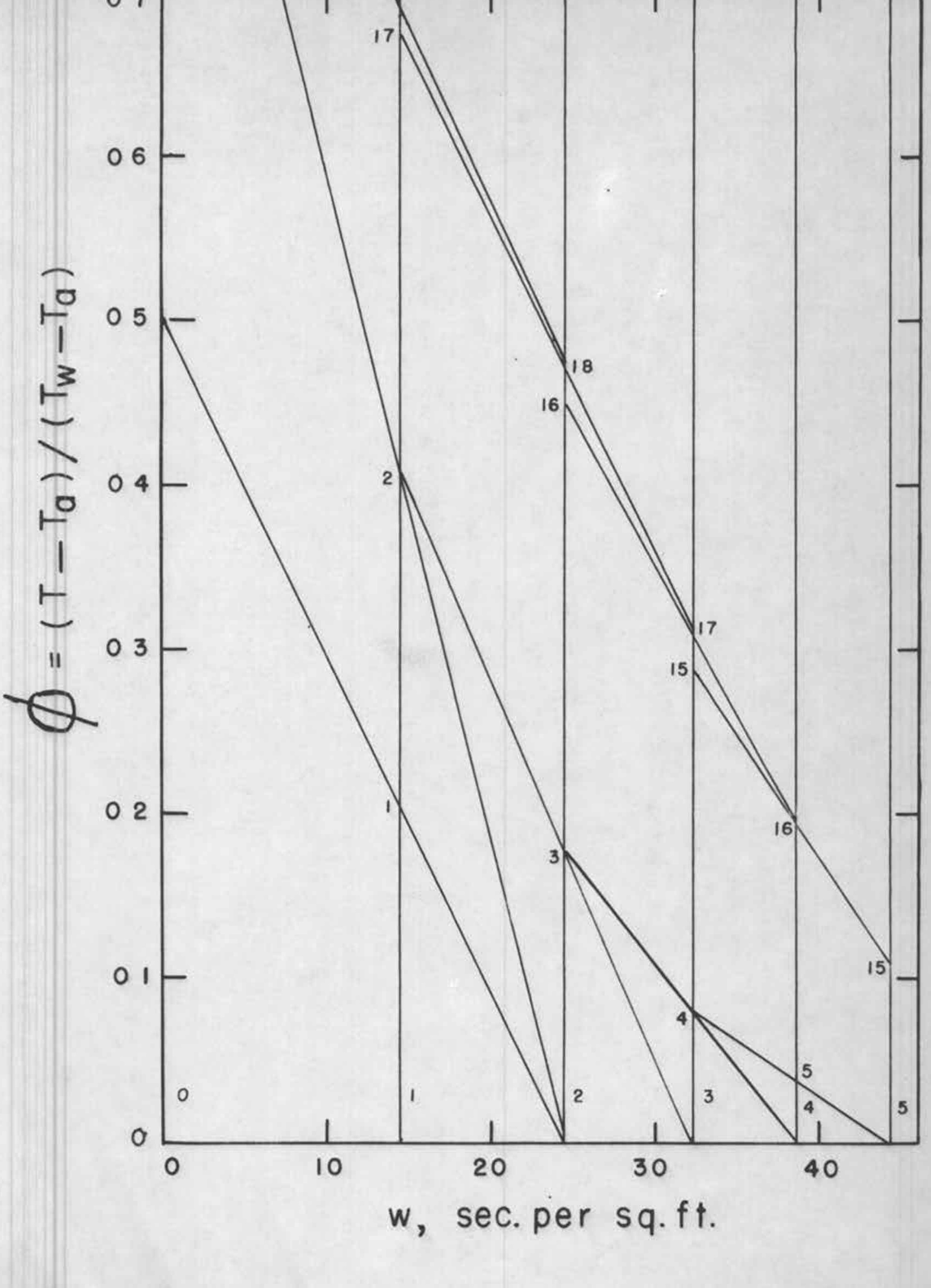

FIGURE 17 GRAPHICAL CONSTRUCTION

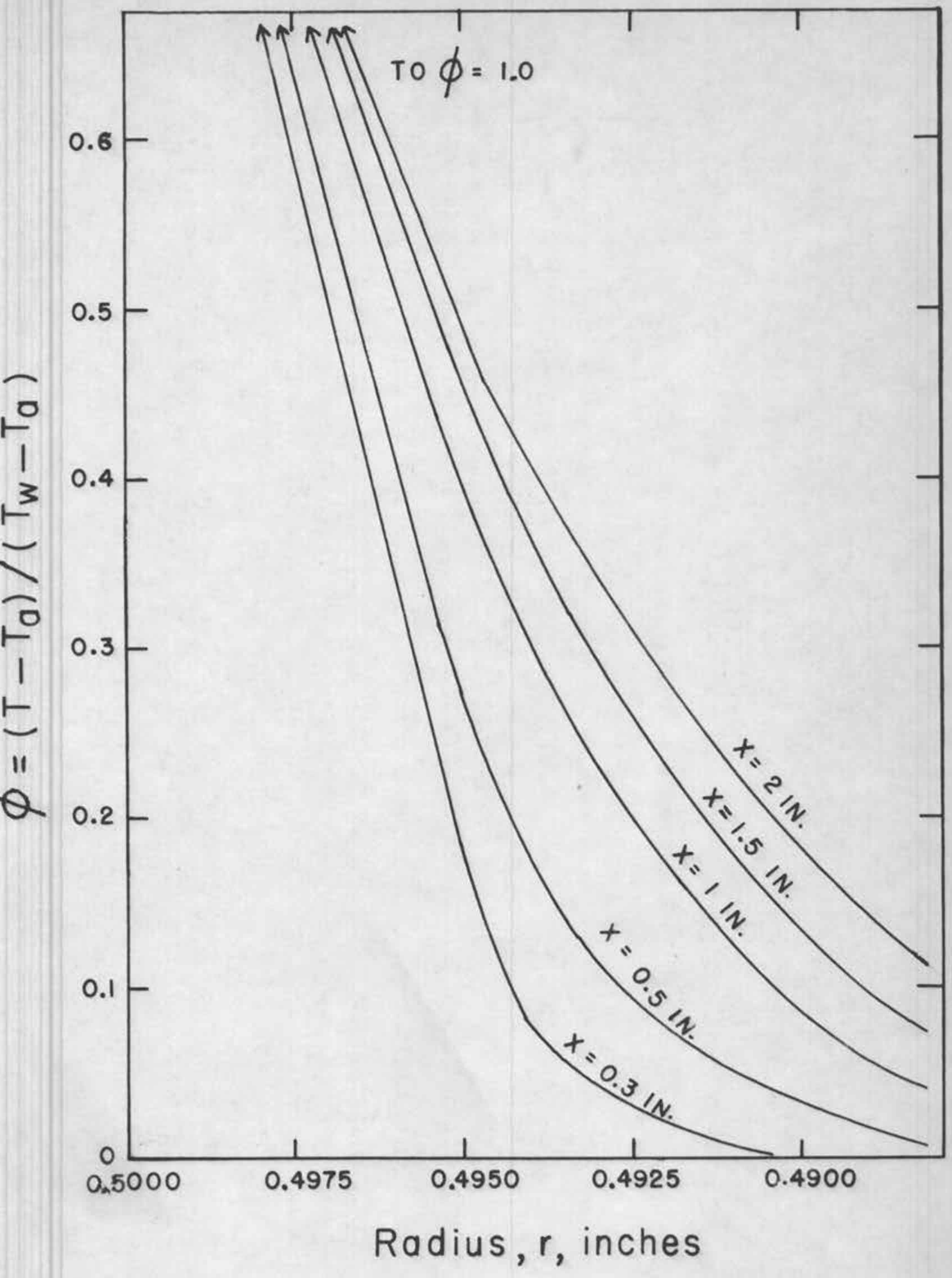

FIGURE 18 TEMPERATURE PROFILE

APPENDIX II

OBSERVED DATA

NOMENCLATURE USED IN TABLE (8)

ΔH : Deflection of orifice manometer, ins. of 0.83 sp. gr. liquid.

I : Current to heating wire, amps.

P_e : Pressure at test section, p.s.i.a.

P_o : Pressure at orifice, p.s.i.a.

T_a : Temperature of entering air, $^{\circ}$ F.

T_{w1}, T_{w2}, T_{w3}, T_{w4}: Temperatures of the inside wall of the heated section at various points.

V : Voltage drop across heating wire, Volts.

In all runs, except for those marked with an asterisk (*), the 0.75 inch orifice was used to measure the flow rate. In runs marked with an asterisk (*), the 1.25 inch orifice was used.

TABLE 8

2 inch Test Section. No Disturber. Group 1

No.	ΔH	T_a	T_{w1}	T_{w2}	T_{w3}	T_{w4}	P_o	P_e	I	V
1	1.26	72.4	127.2	128.0	127.2	128.0	17.3	14.7	0.190	43.0
2	2.20	70.6	130.1	131.2	130.0	130.1	17.3	14.7	0.210	47.0
3	4.31	69.9	125.9	127.0	125.9	126.0	17.2	14.7	0.225	50.8
4	8.03	66.4	125.5	127.3	125.5	126.0	17.2	14.7	0.250	56.9
5	15.6	62.6	127.3	129.3	127.2	128.1	16.8	14.7	0.288	65.6
6	28.9	54.5	123.9	124.5	123.5	125.4	18.1	14.7	0.333	75.0
7*	6.20	53.0	124.0	125.5	123.9	125.5	18.6	14.7	0.382	84.9
8*	12.2	49.0	122.0	123.3	122.0	124.7	23.1	14.7	0.431	99.0
9	1.30	70.2	127.1	128.0	126.8	126.7	17.2	14.6	0.191	43.1
10	2.59	68.0	124.5	126.8	124.5	125.5	17.2	14.6	0.210	46.9
11	4.73	65.1	128.2	129.9	128.2	128.6	17.2	14.6	0.234	52.2
12	8.60	62.2	126.8	128.7	126.8	127.4	17.2	14.6	0.260	58.9
13	15.8	59.3	125.0	126.6	124.9	126.0	17.1	14.6	0.287	64.8
14	28.3	57.3	176.1	126.8	126.1	128.0	17.2	14.6	0.320	73.6
15*	5.20	58.0	124.5	126.0	124.5	127.0	17.8	14.6	0.349	79.9
16*	10.0	52.1	122.6	123.6	122.6	125.6	20.0	14.6	0.404	92.5
17	1.40	75.0	131.1	131.7	129.7	--	17.5	14.7	0.191	43.1
18	2.27	73.6	128.7	130.1	130.0	--	17.5	14.7	0.206	46.3
19	4.10	71.1	129.9	130.9	129.7	--	17.3	14.7	0.224	50.9
20	6.50	70.5	129.6	130.1	129.1	--	17.3	14.7	0.243	55.0
21	10.7	66.6	129.1	130.1	129.6	--	17.2	14.7	0.265	60.1
22	18.7	63.5	129.6	130.1	129.9	--	17.0	14.7	0.290	66.5
23	26.4	61.8	127.4	129.4	128.5	--	17.1	14.7	0.303	69.7
24*	4.10	63.0	128.3	129.5	128.9	--	16.8	14.7	0.327	74.8
25*	6.18	62.6	128.3	130.3	129.8	--	18.1	14.7	0.361	83.0

2 inch Test Section. 1/4 inch Nozzle. Group 2

No.	ΔH	T_a	T_{w1}	T_{w2}	T_{w3}	T_{w4}	P_o	P_e	I	V
1	0.99	74.6	128.5	129.0	128.5	128.5	17.6	14.7	0.296	67.0
2	2.03	72.4	126.4	127.3	127.2	127.0	18.6	14.7	0.342	78.3
3	2.80	70.6	126.3	127.3	126.5	127.1	20.8	14.7	0.278	86.0
4	1.00	74.6	128.1	129.1	128.6	128.6	17.6	14.7	0.314	71.7
5	1.75	73.0	127.7	129.1	128.6	128.6	18.6	14.7	0.350	80.0
6	2.65	71.3	127.4	129.3	128.4	128.8	21.2	14.7	0.383	88.0
7	1.02	75.5	126.8	127.3	127.2	127.2	17.6	14.7	0.308	70.0
8	1.82	73.3	128.5	129.7	129.3	129.6	18.6	14.7	0.350	80.0
9	2.77	71.3	128.3	129.5	129.1	129.5	21.2	14.7	0.381	87.4
10	1.02	76.0	130.0	130.5	130.0	130.0	17.6	14.7	0.251	57.1
11	1.80	73.5	129.3	129.9	129.6	129.6	18.6	14.7	0.278	63.1
12	2.70	71.9	127.5	128.3	128.0	128.2	21.2	14.7	0.295	67.0
13	1.00	77.4	129.1	129.8	129.3	128.8	17.6	14.7	0.210	47.2
14	1.75	73.3	129.5	130.7	129.7	129.7	18.6	14.7	0.230	52.0
15	2.67	71.4	129.5	130.8	129.8	129.8	21.3	14.7	0.250	56.9
16	1.00	74.0	128.6	128.8	128.7	128.2	17.6	14.7	0.199	44.8
17	1.80	72.2	127.2	128.0	127.4	127.0	18.6	14.7	0.212	48.1
18	2.70	70.1	127.4	127.8	127.5	127.2	21.2	14.7	0.232	53.0
19	1.03	74.7	130.0	130.2	129.9	129.6	17.6	14.7	0.185	42.0
20	1.80	72.0	128.7	129.2	128.8	128.6	18.6	14.7	0.199	44.8
21	2.73	70.5	128.2	128.7	128.3	128.2	21.3	14.7	0.212	48.2

2 inch Test Section. 1/2 inch Nozzle. Group 3

No.	ΔH	T_a	T_{w1}	T_{w2}	T_{w3}	T_{w4}	P_o	P_e	I	V
1	1.18	75.2	129.6	130.6	129.9	129.6	17.5	14.7	0.246	55.3
2	2.23	73.7	128.1	129.6	128.3	128.5	17.5	14.7	0.276	62.8
3	4.19	70.4	128.7	129.6	129.2	128.5	17.5	14.7	0.310	71.0
4	7.07	67.6	127.5	129.7	128.6	128.7	17.3	14.7	0.349	80.0
5	11.0	65.2	129.5	130.5	129.6	129.4	17.3	14.7	0.382	88.0
6	18.8	63.1	127.7	129.5	129.2	128.5	18.0	14.7	0.425	98.0
7	28.0	61.5	127.9	129.5	128.9	128.5	19.9	14.7	0.458	105.5
8	1.20	74.5	128.5	129.1	128.5	128.3	17.6	14.8	0.267	60.6
9	2.37	71.8	129.9	130.9	130.3	130.5	17.4	14.8	0.306	69.9
10	4.14	69.6	128.8	130.0	129.0	129.8	17.4	14.8	0.337	77.1
11	7.02	67.6	128.7	129.8	130.2	129.8	17.2	14.8	0.380	85.0
12	11.1	65.5	130.0	130.7	130.2	130.8	17.2	14.8	0.409	94.8
13	18.5	63.1	--	128.7	128.6	129.0	18.1	14.8	0.439	101.0
14	27.6	61.5	--	129.8	130.1	130.4	20.0	14.8	0.479	111.0
15	1.10	75.0	128.8	129.5	128.4	128.7	17.5	14.7	0.268	60.8
16	2.22	73.0	129.7	130.8	129.5	130.2	17.3	14.7	0.300	68.8
17	4.15	70.0	129.5	130.5	130.0	130.2	17.3	14.7	0.333	76.6
18	6.52	68.9	128.6	129.7	129.3	129.6	17.3	14.7	0.367	83.6
19	10.9	65.4	126.0	128.5	129.1	128.5	17.3	14.7	0.399	91.0
20	18.5	62.1	126.5	128.3	128.6	128.6	18.0	14.7	0.439	100.8
21	27.9	61.0	127.2	128.5	128.5	129.5	19.9	14.7	0.473	109.0

Group 3 (Continued)

No.	ΔH	T_a	T_{w1}	T_{w2}	T_{w3}	T_{w4}	P_o	P_e	I	V
22	1.11	74.8	128.2	129.5	128.7	128.7	17.5	14.7	0.238	53.7
23	2.08	72.5	129.8	130.9	130.0	130.1	17.3	14.7	0.261	59.3
24	4.11	69.5	129.8	131.0	130.5	130.5	17.3	14.7	0.291	66.6
25	6.38	67.8	129.8	130.9	130.4	130.6	17.2	14.7	0.312	71.9
26	10.73	65.7	--	129.5	129.0	128.9	17.3	14.7	0.337	77.2
27	18.7	61.7	127.8	129.1	130.4	129.1	18.0	14.7	0.373	85.4
28	27.7	61.4	128.9	129.6	129.2	129.9	19.9	14.7	0.415	95.0
29	1.20	75.2	130.1	130.6	129.1	129.9	17.5	14.7	0.208	47.1
30	2.15	74.0	130.6	130.8	130.6	130.5	17.5	14.7	0.222	50.9
31	4.07	71.0	130.2	130.7	130.0	130.2	17.3	14.7	0.249	56.9
32	6.52	68.3	130.0	130.9	130.6	130.5	17.3	14.7	0.270	61.9
33	10.4	69.0	129.9	131.0	129.0	--	17.3	14.7	0.292	66.5
34	17.7	63.5	128.9	130.1	129.6	129.9	17.9	14.7	0.323	74.0
35	27.6	60.8	--	131.0	130.0	131.0	19.9	14.7	0.362	83.0
36	1.23	74.5	130.2	130.4	130.0	129.8	17.6	14.7	0.199	44.7
37	2.12	72.5	129.0	--	129.2	128.9	17.5	14.7	0.212	48.0
38	4.10	68.7	129.8	130.4	129.3	129.8	17.3	14.7	0.237	54.0
39	6.62	66.0	130.2	130.9	128.7	130.5	17.3	14.7	0.259	59.1
40	10.7	64.2	129.8	130.6	129.6	130.1	17.2	14.7	0.280	64.1
41	17.8	61.7	129.8	131.3	130.9	130.9	17.9	14.7	0.310	71.0
42	27.8	60.0	129.0	130.9	129.7	130.6	19.9	14.7	0.340	78.2
43	1.35	75.0	130.9	131.1	131.0	130.1	17.5	14.7	0.189	43.5
44	2.06	73.4	131.0	131.3	130.9	130.9	17.5	14.7	0.200	45.2
45	4.13	70.1	129.6	130.4	129.9	129.9	17.3	14.7	0.221	50.1

Group 3 (Continued)

No.	ΔH	T_a	T_{w1}	T_{w2}	T_{w3}	T_{w4}	P_o	P_e	I	V
46	6.63	67.3	129.1	129.8	129.4	129.6	17.3	14.7	0.242	55.1
47	10.7	65.0	128.6	129.8	129.6	129.6	17.2	14.7	0.266	60.9
48	18.0	62.5	129.6	130.5	130.1	130.1	17.9	14.7	0.298	68.0
49	27.5	60.9	129.8	130.6	130.1	130.0	19.9	14.7	0.324	74.7
50	1.27	75.4	129.5	130.1	129.8	128.6	17.6	14.7	0.188	42.0
51	2.21	73.5	128.7	130.9	129.8	129.8	17.5	14.7	0.202	45.9
52	4.24	70.0	129.2	130.4	129.1	129.2	17.3	14.7	0.223	50.7
53	6.68	67.0	129.2	130.8	129.5	129.5	17.3	14.7	0.243	55.3
54	10.6	65.0	128.4	130.1	129.2	129.2	17.2	14.7	0.263	60.2
55	18.5	63.0	127.9	129.8	128.4	128.7	18.0	14.7	0.292	67.0
56	27.4	61.0	--	130.8	129.5	129.8	19.9	14.7	0.321	73.9
57	1.25	75.7	129.6	130.5	129.6	128.7	17.5	14.7	0.188	42.5
58	2.23	74.4	129.5	130.6	129.8	129.3	17.5	14.7	0.201	46.7
59	4.11	71.6	128.5	130.3	129.8	128.5	17.5	14.7	0.219	49.4
60	6.70	69.6	128.4	130.2	128.4	128.9	17.3	14.7	0.240	54.1
61	10.6	68.2	128.4	130.3	128.4	124.0	17.3	14.7	0.260	59.2
62	17.1	66.6	128.2	130.5	128.3	129.0	18.0	14.7	0.283	64.7
63	29.4	64.5	128.0	129.0	128.4	128.5	19.9	14.7	0.313	71.9

2 inch Test Section. 1/4 inch Orifice. Group 4

No.	ΔH	T_a	T_{w1}	T_{w2}	T_{w3}	T_{w4}	P_o	P_e	I	V
1	1.01	74.6	128.4	129.6	129.1	128.5	17.5	14.7	0.311	71.0
2	1.43	73.0	128.4	130.8	129.5	129.9	18.6	14.7	0.336	76.9
3	2.23	70.6	129.4	129.6	130.0	130.2	21.3	14.7	0.380	85.2
4	1.00	73.9	127.8	129.0	127.3	128.1	17.5	14.7	0.306	69.2
5	1.42	72.6	126.4	129.1	128.4	128.2	18.3	14.7	0.325	74.7
6	2.26	70.6	--	128.5	127.3	127.9	21.3	14.7	0.363	83.5
7	1.06	75.9	126.5	128.7	128.9	128.0	17.5	14.7	0.321	73.6
8	1.44	74.4	126.6	128.6	--	127.5	18.6	14.7	0.340	77.9
9	2.33	71.5	127.3	128.8	128.1	128.0	21.3	14.7	0.382	87.3
10	1.02	74.4	127.6	129.6	128.5	128.7	17.6	14.8	0.271	62.0
11	1.40	73.1	126.8	129.4	128.6	128.4	18.7	14.8	0.282	64.8
12	2.25	71.2	127.3	128.7	128.7	128.4	21.4	14.8	0.311	71.2
13	1.00	77.2	128.4	129.5	128.4	128.6	17.6	14.8	0.211	48.0
14	1.38	75.0	128.7	130.4	129.2	129.5	18.7	14.8	0.225	51.0
15	2.20	72.6	128.7	130.5	129.2	129.6	21.4	14.8	0.243	55.3
16	1.00	75.1	127.2	128.6	127.6	127.5	17.6	14.8	0.186	41.9
17	1.36	74.2	127.2	128.6	127.7	127.8	18.7	14.8	0.195	44.1
18	2.22	72.3	129.0	130.5	130.0	129.6	21.4	14.8	0.216	49.0
19	1.08	76.0	130.7	131.2	130.5	130.3	17.5	14.7	0.182	41.1
20	1.40	74.1	130.9	131.7	130.8	130.8	18.6	14.7	0.184	42.9
21	2.16	73.5	130.8	131.6	130.8	130.8	21.3	14.7	0.206	46.5

2 inch Test Section. 1/2 inch Orifice. Group 5

No.	ΔH	T_a	T_{w1}	T_{w2}	T_{w3}	T_{w4}	P_o	P_e	I	V
1	1.22	74.9	128.4	130.4	128.9	129.0	17.4	14.6	0.265	60.1
2	2.12	72.5	128.3	130.0	129.6	130.0	17.4	14.6	0.297	67.8
3	4.09	69.5	128.3	129.7	129.1	129.2	17.3	14.6	0.336	77.0
4	6.62	67.4	128.0	129.3	128.6	128.7	17.2	14.6	0.371	84.8
5	10.4	64.1	127.8	129.2	128.5	129.2	17.1	14.6	0.408	92.9
6	16.6	61.5	--	129.2	127.7	127.7	18.5	14.6	0.441	101.0
7	26.5	57.5	127.7	129.5	127.9	127.9	21.2	14.6	0.48	112.2
8	1.32	73.5	129.8	131.1	130.1	130.1	17.4	14.6	0.281	64.0
9	2.32	70.5	129.0	129.3	128.9	129.1	17.4	14.6	0.313	71.9
10	4.02	67.4	127.2	128.4	128.1	128.2	17.3	14.6	0.348	79.0
11	6.70	65.0	127.0	128.5	127.1	127.0	17.3	14.6	0.381	87.0
12	10.3	63.5	127.3	128.4	127.1	--	17.2	14.6	0.410	93.6
13	16.9	61.0	127.2	129.0	127.6	127.3	18.5	14.6	0.450	103.0
14	26.6	59.3	129.3	130.9	129.9	129.4	21.2	14.6	0.499	115.1
15	1.26	73.9	129.1	131.2	130.2	130.1	17.5	14.7	0.281	63.9
16	2.21	71.3	128.7	130.1	129.0	128.9	17.5	14.7	0.310	71.0
17	4.02	68.4	128.7	129.2	129.0	129.1	17.4	14.7	0.346	79.0
18	6.55	66.1	127.6	129.7	127.9	127.9	17.3	14.7	0.376	85.7
19	10.6	63.4	127.6	129.2	127.6	127.6	17.3	14.7	0.410	93.8
20	16.9	60.9	127.0	128.8	127.5	127.0	18.6	14.7	0.447	102.3
21	26.7	58.9	127.8	129.2	127.8	127.3	21.3	14.7	0.490	113.1
22	1.35	74.1	127.6	129.2	128.1	127.9	17.5	14.7	0.248	55.9
23	2.35	71.6	129.5	130.5	129.5	129.8	17.5	14.7	0.272	61.9
24	4.06	69.0	127.5	129.8	128.9	128.5	17.5	14.7	0.297	67.3
25	6.60	66.6	128.3	129.6	128.5	128.5	17.4	14.7	0.322	74.0
26	10.3	69.5	127.9	130.0	129.8	128.4	17.3	14.7	0.342	78.3

Group 5 (Continued)

No.	ΔH	T_a	T_{w1}	T_{w2}	T_{w3}	T_{w4}	P_o	P_e	I	V
27	16.7	62.5	127.6	129.7	129.0	127.9	18.6	14.7	0.380	88.0
28	26.4	59.1	--	128.3	128.8	128.3	21.3	14.7	0.422	97.0
29	1.29	74.7	128.7	130.0	--	129.0	17.4	14.6	0.206	46.4
30	2.37	72.4	128.6	129.9	--	129.0	17.4	14.6	0.223	50.7
31	4.08	69.5	128.3	129.7	--	128.6	17.3	14.6	0.246	55.9
32	6.50	66.2	127.1	129.1	--	128.0	17.2	14.6	0.276	60.7
33	10.3	67.4	128.1	128.6	--	128.0	17.2	14.6	0.291	66.3
34	16.8	61.4	127.6	128.5	--	127.8	18.5	14.6	0.323	74.8
35	26.7	58.0	128.9	129.1	--	128.6	21.2	14.6	0.360	82.3
36	1.31	69.4	128.4	129.7	--	128.4	17.4	14.6	0.193	44.0
37	2.32	69.9	128.5	129.8	--	128.8	17.4	14.6	0.210	47.8
38	4.05	68.3	128.2	129.7	--	128.8	17.3	14.6	0.229	52.0
39	6.52	65.4	128.0	129.8	--	128.8	17.2	14.6	0.250	56.9
40	11.1	62.5	127.4	129.2	--	128.0	17.1	14.6	0.273	62.2
41	16.9	60.0	127.2	129.2	--	128.0	18.5	14.6	0.301	68.8
42	26.7	57.3	128.4	129.4	--	128.3	21.2	14.6	0.331	76.2
43	1.36	76.7	128.4	128.9	--	128.3	17.3	14.5	0.187	42.0
44	2.26	73.2	128.3	128.9	--	178.3	17.3	14.5	0.200	45.0
45	4.05	71.2	129.8	131.1	--	129.8	17.3	14.5	0.227	51.0
46	6.55	65.6	129.4	131.2	--	129.8	17.2	14.5	0.246	55.5
47	11.1	62.2	129.3	129.7	--	129.4	17.0	14.5	0.269	61.0
48	16.7	60.3	128.1	129.7	--	129.1	18.4	14.5	0.292	66.3
49	26.7	57.3	128.1	128.5	--	128.7	21.1	14.5	0.321	73.4

1 inch Test Section. No Disturber. Group 6

No.	ΔH	T_a	T_{w1}	T_{w2}	T_{w3}	T_{w4}	P_o	P_e	I	V
1	1.25	70.0	130.5	130.6	129.7	131.0	17.6	14.7	0.271	25.1
2	2.27	67.8	129.9	124.9	130.0	130.1	17.5	14.7	0.288	27.0
3	4.07	65.0	129.9	129.9	130.0	130.1	17.5	14.7	0.314	29.0
4	6.60	62.9	129.2	129.3	129.8	129.7	17.3	14.7	0.332	31.0
5	10.8	61.0	130.3	130.4	130.6	130.4	17.3	14.7	0.361	34.0
6	17.0	59.4	130.2	130.3	131.6	130.5	17.2	14.7	0.391	36.5
7*	4.40	56.0	129.1	129.1	131.0	129.1	17.2	14.7	0.446	42.0
8*	6.10	54.7	129.4	129.8	131.0	129.8	18.2	14.7	0.474	44.9
9	1.45	71.2	128.8	128.9	129.2	129.2	17.6	14.7	0.266	25.0
10	2.35	69.5	128.9	128.9	129.7	129.3	17.5	14.7	0.272	26.1
11	4.15	66.5	127.3	127.7	128.8	127.8	17.4	14.7	0.296	28.1
12	6.90	63.6	127.9	127.8	128.9	127.9	17.3	14.7	0.323	30.5
13	11.3	61.6	127.9	128.1	129.1	127.9	17.2	14.7	0.360	33.3
14	20.2	59.6	130.0	131.1	131.7	131.2	17.1	14.7	0.399	37.9
15*	4.11	57.0	128.2	128.4	129.7	128.5	17.0	14.7	0.434	41.8
16*	6.15	54.1	128.2	127.5	--	128.9	18.2	14.7	0.468	45.0
17	1.45	70.1	128.5	128.5	129.6	128.9	17.7	14.8	0.262	24.7
18	2.30	68.5	129.3	129.3	130.3	129.7	17.6	14.8	0.278	26.0
19	4.05	65.5	129.2	129.4	131.0	129.6	17.5	14.8	0.304	28.3
20	6.90	62.6	129.4	129.4	131.0	129.4	17.4	14.8	0.330	31.3

Group 6 (Continued)

No.	ΔH	T_a	T_{w1}	T_{w2}	T_{w3}	T_{w4}	P_o	P_e	I	V
21	10.7	60.5	129.7	130.7	131.0	129.6	17.4	14.8	0.356	34.0
22	18.9	57.9	128.9	130.2	--	130.4	17.3	14.8	0.391	37.2
23*	3.95	56.0	129.3	129.7	131.0	129.1	17.1	14.8	0.439	41.5
24*	6.15	53.5	129.5	129.0	130.5	129.5	18.3	14.8	0.478	45.5
25	1.56	69.2	129.7	129.8	131.8	130.2	17.7	14.8	0.266	25.0
26	2.30	67.2	130.3	130.3	132.0	130.9	17.6	14.8	0.284	27.0
27	4.12	64.8	127.9	127.9	129.0	127.9	17.5	14.8	0.299	28.5
28	6.90	62.3	127.9	127.9	129.2	128.1	17.4	14.8	0.324	31.1
29	11.0	60.4	130.5	130.5	131.8	130.2	17.4	14.8	0.360	34.2
30	18.9	58.2	130.6	130.5	132.6	130.5	17.3	14.8	0.382	36.5

1 inch Test Section. 1/2 inch Nozzle. Group 7

No.	ΔH	T_a	T_{w1}	T_{w2}	T_{w3}	T_{w4}	P_o	P_e	I	V
1	1.38	68.9	128.5	129.0	128.5	129.0	17.5	14.7	0.324	36.4
2	2.37	66.6	126.3	126.5	126.3	126.5	17.5	14.7	0.353	39.9
3	4.08	66.4	129.8	129.3	129.3	129.8	17.5	14.7	0.435	41.7
4	6.78	62.4	128.5	127.7	128.2	128.5	17.5	14.7	0.475	45.9
5	10.6	59.3	129.6	128.9	129.3	129.5	17.4	14.7	0.520	50.0
6	16.8	57.2	129.3	128.5	129.1	129.4	17.5	14.7	0.565	54.2
7	27.3	55.5	128.2	--	128.4	128.9	19.2	14.7	0.616	59.4
8	1.40	71.0	129.8	129.6	128.9	129.8	17.7	14.8	0.362	34.3
9	2.30	68.6	130.0	129.5	128.9	130.0	17.6	14.8	0.392	37.4
10	4.12	65.8	127.5	127.3	127.1	127.5	17.5	14.8	0.426	40.8
11	6.92	63.0	128.5	127.7	127.4	128.1	17.4	14.8	0.468	44.9
12	10.6	60.6	128.5	128.0	127.9	128.4	17.3	14.8	0.509	48.7
13	16.9	58.3	130.6	129.9	129.9	130.3	17.4	14.8	0.559	53.5
14	27.9	55.9	128.5	127.3	127.7	128.0	19.4	14.8	0.605	57.8
15	1.48	70.0	129.8	129.8	128.9	129.9	17.5	14.7	0.351	33.7
16	2.32	67.4	129.7	129.6	128.9	129.8	17.5	14.7	0.375	35.9
17	4.14	65.0	129.7	128.9	128.9	129.7	17.4	14.7	0.410	39.7
18	6.85	62.7	129.0	128.1	129.0	129.0	17.3	14.7	0.443	42.6
19	10.9	60.2	128.6	128.0	127.8	128.6	17.2	14.7	0.476	46.0
20	17.7	58.2	128.6	127.7	127.4	128.5	17.5	14.7	0.516	49.9
21	28.5	56.6	128.2	127.1	127.1	128.5	19.4	14.7	0.569	54.9
22	1.41	68.1	129.6	129.6	128.9	129.6	17.4	14.6	0.307	29.2
23	2.32	67.5	129.6	129.5	128.9	129.6	17.4	14.6	0.324	30.9
24	4.07	65.6	129.5	129.3	128.6	129.3	17.3	14.6	0.351	33.4
25	6.80	62.7	129.9	129.8	129.5	129.9	17.2	14.6	0.383	36.6

Group 7 (Continued)

No.	ΔH	T_a	T_{w1}	T_{w2}	T_{w3}	T_{w4}	P_o	P_e	I	V
26	10.6	60.0	128.9	128.4	128.4	128.7	17.1	14.6	0.409	39.1
27	18.3	58.0	128.1	127.6	127.5	128.1	17.5	14.6	0.444	42.5
28	28.7	56.0	128.0	128.5	128.3	128.0	19.4	14.6	0.485	46.5
29	1.45	68.2	129.6	129.7	128.9	129.6	17.4	14.6	0.287	27.7
30	2.38	67.1	128.8	129.2	129.5	129.2	17.4	14.6	0.303	29.0
31	4.16	65.0	128.6	128.7	128.4	128.7	17.3	14.6	0.324	30.9
32	6.94	61.9	127.6	127.4	127.2	127.5	17.2	14.6	0.346	33.2
33	10.8	60.1	127.9	127.5	127.2	127.4	17.1	14.6	0.374	36.0
34	18.4	58.2	127.4	127.2	127.0	127.4	17.5	14.6	0.400	38.1
35	28.2	56.8	218.2	127.2	127.2	128.2	19.4	14.6	0.445	43.0

APPENDIX III

CALCULATED DATA

CALCULATED DATA

Sample Calculation

A sample calculation is given below showing the steps followed in calculating the Nusselt and Reynolds numbers for run number 18 of Group 1.

Calculation of Nu

$$q = (0.206)\ (46.3) \text{ watts} = \frac{(0.206)\ (46.3)}{(0.293)} \ \frac{\text{BTU}}{\text{hr}}$$

$$= 32.6 \text{ BTU/hr.}$$

$$A_W = 0.0436 \text{ sq. ft.}$$

$$(T_W - T_a) = 56.2 \ {}^{o}\text{F}$$

$$h = \frac{q}{A_W\ (T_W - T_a)} = \frac{32.6}{(0.0436)(56.2)} = 13.3 \text{ BTU/hr.}$$

$$\text{sq.ft. } {}^{o}\text{F.} \quad Nu = \frac{hD}{k} = \frac{13.3}{(0.015)(12)} = 73.9$$

$$\underline{Nu = 73.9}$$

Calculation of Re

From Ambrose's calibration curve (1, P. 163) for $\Delta H = 2.27$, $\frac{Q\ \rho_e}{(\rho_o)^{1/2}}$ after applying a 3 per cent correction is equal to 2.90.

ρ_o = 0.0887 lbs/cu.ft. and ρ_e = 0.0745 lbs/cu.ft.

So $Q = \frac{(2.9)(0.0887)^{1/2}}{0.0745}$ 11.6 cu.ft./min.

From equation (33) $Re = \frac{BQ}{\mu}$ where

$$B = \frac{(60)(D)(\rho_{60})}{A_c}$$, a constant.

$$B = \frac{(60)(0.0754)}{(12)(0.00546)} = 69.0 \ \frac{\text{lbs}}{\text{cu.ft.}} \ \frac{\text{min.}}{\text{hr}} \ \frac{1}{\text{ft}}$$

μ at 74° F = 0.0441 $\frac{\text{lbs}}{\text{ft-hr}}$

So $Re = \frac{69 \times 11.6}{0.0441} = 1.816 \times 10^4$

$$\underline{Re = 1.82 \times 10^4}$$

Nomenclature used in Table (9)

h	:	Average heat transfer coefficient BTU/(hr) (sq.ft.) (^{o}F).
l	:	Distance of disturber from upstream end of heated section.
Nu	:	Average Nusselt number, $\frac{hD}{k}$
Q	:	Air flow rate, cu.ft./min. measured at 60° F and 1 atmosphere pressure.
q	:	Amount of heat transferred, BTU/hr.
T_a	:	Temperature of entering air, ^{o}F.
T_w	:	Average temperature of inside wall of heated section.

TABLE 9

2 inch Test Section. No Disturber.

Group 1

No.	$(T_w - T_a)$	Q	q	h	$Re x 10^{-4}$	Nu	ℓ
1	55.0	8.55	27.9	11.6	1.33	64.4	--
2	59.6	11.3	34.9	13.4	1.76	74.3	--
3	56.2	15.8	39.0	15.9	2.46	88.0	--
4	59.3	21.6	48.6	18.8	3.40	104.3	--
5	64.9	29.6	64.5	22.6	4.67	126.5	--
6	70.0	41.9	84.5	27.6	6.70	153.2	--
7	71.7	59.8	110.6	35.3	9.60	195.9	--
8	74.0	92.4	141.0	41.1	14.90	228.1	--
9	56.8	8.67	28.2	11.4	1.36	63.1	--
10	56.9	12.3	33.6	13.5	1.92	75.0	--
11	63.3	16.5	41.7	15.1	2.44	83.8	--
12	64.8	22.3	52.9	18.7	3.52	103.8	--
13	66.0	29.8	63.5	22.0	4.74	122.1	--
14	69.4	40.4	80.5	26.6	6.44	147.6	--
15	67.5	58.5	95.1	32.3	9.30	179.3	--
16	71.5	79.0	127.3	40.9	12.68	227.0	--
17	56.1	9.11	28.2	11.5	1.42	63.8	--
18	56.2	11.6	32.6	11.3	1.82	73.7	--
19	59.0	15.5	39.0	15.1	2.42	83.9	--
20	59.1	19.5	45.6	17.7	3.06	98.0	--
21	63.0	25.0	54.5	19.8	3.94	110.0	--
22	66.4	32.7	66.0	22.8	5.16	126.5	--
23	66.9	39.1	72.1	25.4	6.18	141.0	--
24	65.7	47.0	83.5	29.1	7.40	161.5	--
25	67.2	59.9	102.2	33.8	9.45	187.6	--

2 inch Test Section. 1/4 inch Nozzle.

Group 2

No.	$(T_w - T_a)$	Q	q	h	Rex10^{-4}	Nu	ℓ
1	54.0	7.70	67.6	28.7	1.20	159.3	0
2	54.7	11.3	91.4	38.2	1.76	212.0	0
3	56.2	14.1	111.0	45.2	2.19	250.9	0
4	54.0	7.74	76.9	32.4	1.20	179.8	0.5
5	55.3	10.5	95.5	39.6	1.63	219.8	0.5
6	57.0	13.8	115.0	46.2	2.15	256.4	0.5
7	51.6	7.79	73.6	32.6	1.22	180.9	1
8	56.1	10.6	95.6	39.0	1.66	216.5	1
9	57.7	13.9	113.6	45.1	2.17	250.3	1
10	54.1	7.80	49.0	20.7	1.21	114.9	3
11	56.1	10.6	59.9	24.4	1.65	135.4	3
12	56.1	14.1	67.5	27.5	2.20	152.6	3
13	51.8	7.74	33.8	15.0	1.19	83.1	5
14	56.5	10.5	40.9	16.5	1.63	91.7	5
15	58.4	13.9	48.5	19.4	2.16	107.4	5
16	54.6	7.74	30.4	12.7	1.20	70.5	7
17	55.4	10.6	34.8	14.4	1.65	79.9	7
18	57.4	13.9	42.0	16.8	2.18	93.2	7
19	55.3	7.81	26.6	11.0	1.20	61.1	12
20	56.9	10.6	30.4	12.3	1.65	68.3	12
21	57.8	14.0	34.9	13.9	2.18	77.1	12

2 inch Test Section. 1/2 inch Nozzle.

Group 3

No.	$(T_w - T_a)$	Q	q	h	Rex10^{-4}	Nu	l
1	54.7	8.39	46.4	19.4	1.30	107.7	0
2	54.9	11.5	59.1	24.7	1.79	136.6	0
3	58.7	15.6	75.1	29.3	2.46	162.6	0
4	61.0	20.3	95.4	35.8	3.19	198.7	0
5	64.7	25.2	114.8	40.6	3.98	225.3	0
6	65.6	33.8	142.1	49.6	5.34	275.3	0
7	67.2	43.8	165.0	56.2	6.85	311.5	0
8	54.1	8.42	55.4	23.4	1.31	129.9	0.5
9	58.7	11.8	73.1	28.5	1.84	158.2	0.5
10	59.9	15.5	88.9	34.0	2.56	188.7	0.5
11	62.0	20.1	110.2	40.7	3.16	225.9	0.5
12	65.1	25.2	132.1	46.5	3.98	258.1	0.5
13	65.6	33.6	151.1	52.8	5.30	292.0	0.5
14	68.6	43.0	181.1	60.5	6.80	335.8	0.5
15	53.8	8.05	55.6	23.7	1.25	131.5	1.0
16	57.0	11.1	70.5	28.3	1.77	157.1	1.0
17	60.0	15.5	87.0	33.2	2.43	184.3	1.0
18	60.6	19.5	104.8	39.6	3.05	219.8	1.0
19	62.6	25.2	124.0	45.3	3.97	251.4	1.0
20	65.9	33.6	151.0	52.5	5.31	291.4	1.0
21	67.6	43.1	176.0	59.5	6.85	330.2	1.0
22	53.9	8.08	43.6	18.5	1.26	104.0	3
23	57.6	11.0	52.4	20.8	1.72	115.4	3
24	61.0	15.5	66.6	25.0	2.42	138.8	3
25	62.7	19.3	75.5	27.6	3.03	153.2	3
26	63.4	25.2	89.0	32.1	3.93	178.2	3
27	67.3	33.6	108.7	37.0	5.31	205.4	3
28	68.1	43.0	134.6	45.2	6.81	250.9	3
29	54.8	8.44	33.5	14.0	1.31	77.7	5
30	56.4	11.3	38.5	15.6	1.76	86.7	5
31	59.2	15.5	48.4	18.7	2.42	103.8	5
32	62.2	19.1	57.0	21.0	3.00	116.6	5
33	61.0	24.8	65.3	24.5	3.87	136.0	5
34	66.2	32.7	81.6	28.2	5.16	156.5	5
35	69.9	43.0	102.5	33.6	6.82	186.5	5
36	55.6	8.58	30.4	12.5	1.34	69.3	7
37	56.6	11.2	34.8	14.1	1.75	78.2	7
38	61.2	15.4	43.7	16.4	2.42	91.0	7
39	64.2	19.7	52.4	18.7	3.10	103.0	7
40	65.9	25.0	61.5	21.4	3.95	118.8	7
41	69.1	32.8	75.1	24.8	5.20	137.7	7

Group 3 (Continued)

No.	$(T_w - T_a)$	Q	q	h	Rex10^{-4}	Nu	ℓ
42	70.2	43.0	89.6	29.2	6.83	162.1	7
43	55.7	8.95	28.0	11.5	1.39	63.9	12
44	57.6	11.0	30.8	12.2	1.72	67.8	12
45	69.9	15.5	37.9	14.5	2.42	80.5	12
46	62.2	19.8	44.5	16.4	3.11	91.0	12
47	64.5	25.0	55.2	19.6	3.94	108.8	12
48	67.6	33.0	69.1	23.0	5.22	127.9	12
49	69.2	43.0	82.8	27.3	6.82	151.7	12
50	54.1	8.71	26.9	11.4	1.35	63.2	12
51	56.3	11.5	31.7	12.9	1.78	71.6	12
52	69.5	15.8	38.6	14.8	2.47	82.3	12
53	62.8	19.8	45.9	16.7	3.11	92.7	12
54	64.2	24.8	54.1	19.3	3.91	107.1	12
55	65.8	33.6	66.8	23.2	5.30	128.8	12
56	69.0	42.8	81.0	26.8	6.78	148.7	12
57	54.9	8.60	27.3	11.4	1.34	63.3	50
58	55.4	11.4	32.1	13.3	1.78	73.7	50
59	57.3	1.55	36.9	14.8	2.43	81.9	50
60	59.4	19.8	44.4	17.1	3.09	94.9	50
61	60.9	24.8	52.7	19.8	3.89	110.0	50
62	62.4	31.4	62.5	22.9	4.94	127.3	50
63	64.0	44.0	79.2	28.3	6.94	157.1	50

2 inch Test Section. 1/4 inch Orifice

Group 4

No.	$(T_w - T_a)$	Q	q	h	$Re x 10^{-4}$	Nu	l
1	54.1	7.79	75.4	31.8	1.21	176.5	0
2	56.9	9.46	88.1	35.5	1.49	197.0	0
3	59.4	12.6	110.9	42.7	1.97	237.0	0
4	54.1	7.72	72.9	30.7	1.20	170.4	0.5
5	55.4	9.45	82.9	34.8	1.49	193.1	0.5
6	57.2	12.7	103.3	41.2	1.98	228.7	0.5
7	52.2	7.94	80.7	35.4	1.23	196.5	1
8	53.1	9.54	90.4	38.8	1.49	215.3	1
9	56.6	13.0	113.6	45.9	2.03	254.7	1
10	54.3	7.80	57.4	24.2	1.21	134.3	3
11	55.4	9.37	62.4	25.8	1.46	143.2	3
12	56.9	12.7	75.6	30.4	1.98	168.7	3
13	51.5	7.75	34.5	15.3	1.20	84.9	5
14	54.5	9.34	39.2	16.5	1.45	91.6	5
15	56.9	12.1	45.8	18.4	1.89	102.1	5
16	52.6	7.71	26.4	11.4	1.20	63.5	7
17	53.5	9.26	29.6	12.6	1.44	69.9	7
18	57.6	12.2	36.1	14.4	1.89	80.1	7
19	54.7	8.01	25.4	10.6	1.24	58.8	12
20	57.0	9.38	27.8	11.2	1.46	62.2	12
21	57.6	12.5	32.7	13.0	1.94	71.9	12

2 inch Test Section. 1/2 inch Orifice

Group 5

No.	$(T_w - T_a)$	Q	q	h	Rex10^{-4}	Nu	ℓ
1	54.3	8.50	54.4	22.9	1.32	127.1	0
2	57.1	11.2	68.8	27.5	1.75	152.6	0
3	59.6	15.5	88.5	33.9	2.42	188.1	0
4	61.2	19.7	107.1	40.1	3.10	222.6	0
5	62.6	24.5	129.0	47.1	3.86	261.4	0
6	66.6	32.3	152.0	52.2	5.11	289.7	0
7	70.7	43.5	186.2	60.4	6.94	335.2	0
8	56.8	8.81	61.4	24.7	1.37	137.1	0.5
9	58.6	11.7	76.6	29.9	1.83	165.9	0.5
10	60.7	15.4	93.7	35.3	2.42	195.9	0.5
11	62.5	19.7	113.0	41.5	3.10	230.3	0.5
12	64.0	24.5	131.0	46.9	3.87	260.3	0.5
13	66.6	32.6	158.0	54.3	5.16	301.4	0.5
14	70.6	43.5	196.0	63.6	6.91	353.0	0.5
15	56.3	8.60	61.3	24.9	1.34	138.2	1
16	57.7	11.4	75.0	29.7	1.78	164.8	1
17	60.6	15.4	93.1	35.1	2.42	194.8	1
18	62.0	19.6	110.0	40.6	3.09	225.3	1
19	64.4	24.9	131.0	46.6	3.93	258.6	1
20	66.6	32.6	156.0	53.6	5.16	297.5	1
21	69.3	43.5	188.0	62.2	6.92	345.2	1
22	54.0	8.94	47.1	20.0	1.39	111.0	3
23	58.2	11.7	57.5	22.6	1.83	125.4	3
24	59.7	15.5	68.3	26.2	2.42	145.4	3
25	62.1	19.7	81.3	29.9	3.10	165.9	3
26	59.4	24.5	90.4	34.8	3.78	193.1	3
27	65.9	32.3	114.0	39.6	5.10	219.8	3
28	69.8	43.4	139.8	45.9	6.90	254.7	3
29	54.5	8.71	32.5	13.65	1.36	75.8	5
30	56.7	11.8	38.6	15.6	1.85	86.6	5
31	59.4	15.5	46.9	18.1	2.42	100.5	5
32	61.8	19.5	57.2	21.2	3.06	117.7	5
33	60.6	24.6	66.0	24.9	3.86	138.2	5
34	66.5	32.4	81.5	28.0	5.13	155.4	5
35	70.5	43.5	101.0	32.7	6.94	181.6	5
36	59.4	8.75	79.0	11.2	1.37	62.2	7
37	59.0	11.7	34.2	12.9	1.83	71.6	7

Group 5 (Continued)

No.	$(T_w - T_a)$	Q	q	h	$Re x 10^{-4}$	Nu	l
38	60.6	15.4	40.6	15.35	2.42	85.2	7
39	63.5	19.4	48.5	17.5	3.06	97.1	7
40	65.6	25.2	58.0	20.2	3.98	112.1	7
41	68.0	32.3	70.6	23.8	5.13	132.1	7
42	71.5	43.5	86.0	27.5	6.95	152.6	7
43	51.8	8.95	24.8	11.1	1.38	61.6	12
44	55.3	11.5	30.8	12.8	1.79	71.0	12
45	58.9	15.5	39.5	15.3	2.42	84.9	12
46	64.4	19.5	46.6	17.0	3.08	94.4	12
47	67.2	25.1	56.0	19.8	3.96	109.9	12
48	68.7	32.1	66.1	22.0	5.09	122.1	12
49	71.2	42.9	80.4	25.8	6.82	143.2	12

1 inch Test Section. No Disturber

Group 6

No.	$(T_W - T_a)$	Q	q	h	$Rex10^{-4}$	Nu	ℓ
1	60.5	9.32	23.2	17.5	1.49	97.1	--
2	62.2	11.5	26.5	19.5	1.80	108.2	--
3	65.0	15.4	32.2	22.6	2.43	125.4	--
4	66.6	19.6	35.1	24.1	3.10	133.8	--
5	69.4	25.1	40.5	26.8	3.98	148.7	--
6	71.2	31.2	49.4	31.7	4.95	175.9	--
7	73.5	48.7	64.0	39.9	7.93	221.4	--
8	75.3	58.8	72.5	44.0	9.39	244.2	--
9	57.8	9.28	22.0	17.4	1.45	96.6	--
10	59.7	11.7	24.7	18.9	1.84	104.9	--
11	61.4	15.6	28.4	21.2	2.46	117.7	--
12	64.4	20.0	33.7	24.0	3.16	133.2	--
13	66.6	25.5	40.9	28.0	4.04	155.4	--
14	71.5	34.1	51.1	32.8	5.41	182.0	--
15	71.7	47.0	62.0	39.6	7.50	219.8	--
16	74.1	59.2	71.9	44.4	9.47	246.4	--
17	58.8	9.14	22.0	17.1	1.43	94.9	--
18	61.0	11.6	24.6	18.4	1.82	102.1	--
19	64.2	15.3	29.4	21.0	2.41	116.6	--
20	67.2	19.9	35.3	24.0	3.14	133.2	--
21	69.7	25.0	41.4	27.2	3.96	151.0	--
22	72.1	32.8	49.6	31.5	5.23	174.8	--
23	73.8	45.5	62.1	38.6	7.44	214.2	--
24	76.0	59.0	74.2	44.6	9.45	247.5	--
25	61.1	9.54	22.7	17.0	1.49	94.4	--
26	63.7	11.6	26.2	18.8	1.82	104.3	--
27	63.4	15.4	29.1	21.0	2.43	116.6	--
28	65.9	19.9	34.4	23.9	3.14	132.6	--
29	70.5	25.1	42.0	27.3	3.99	151.5	--
30	72.9	32.8	47.6	30.0	5.23	116.5	--

1 inch Test Section. 1/2 inch Nozzle

Group 7

No.	$(T_w - T_a)$	Q	q	h	$Re \times 10^{-4}$	Nu	l
1	59.9	8.99	40.5	31.0	1.42	172.1	1
2	59.8	11.8	48.0	36.7	1.85	203.7	1
3	63.1	15.3	61.9	44.8	2.40	248.7	1
4	66.0	19.6	74.5	51.6	3.10	286.4	1
5	70.0	24.6	89.0	58.1	3.92	322.5	1
6	71.9	30.9	104.7	66.8	4.93	370.7	1
7	73.0	41.2	125.0	78.5	6.58	435.7	1
8	58.5	9.04	42.4	33.1	1.41	183.7	2
9	61.0	11.5	50.0	37.5	1.81	208.1	2
10	61.6	15.3	59.5	44.1	2.42	244.7	2
11	64.9	19.9	71.6	50.5	3.14	280.3	2
12	67.6	24.6	84.5	57.1	3.90	316.9	2
13	71.8	31.1	102.0	65.0	4.95	360.8	2
14	71.9	41.8	119.0	75.9	6.68	421.2	2
15	59.6	9.30	40.4	30.9	1.47	171.5	3
16	62.1	11.7	46.0	33.8	1.83	187.6	3
17	64.3	15.5	55.2	39.3	2.44	218.1	3
18	65.8	19.9	64.5	44.7	3.14	248.1	3
19	68.0	25.0	72.9	49.0	3.97	272.0	3
20	69.8	32.2	87.5	57.2	5.14	317.5	3
21	71.2	43.0	106.3	68.4	6.86	379.6	3
22	61.4	9.15	30.6	22.8	1.43	126.5	5
23	62.0	11.7	34.3	25.3	1.84	140.4	5
24	64.1	15.4	40.0	28.5	2.44	158.2	5
25	67.1	19.9	47.9	32.2	3.14	178.7	5
26	68.6	24.8	54.6	36.4	3.94	202.0	5
27	69.8	32.8	64.5	42.3	5.10	234.8	5
28	72.2	43.5	77.0	48.8	6.95	270.8	5
29	61.3	9.25	27.2	20.2	1.45	112.1	7
30	61.8	11.9	29.9	22.2	1.87	123.2	7
31	63.6	15.6	34.2	24.5	2.46	136.0	7
32	65.5	20.1	39.2	27.3	3.20	151.5	7
33	67.4	25.0	45.9	31.1	3.95	172.6	7
34	69.0	33.0	50.6	33.6	5.25	186.5	7
35	70.8	42.9	65.2	42.1	6.85	233.7	7

Least square analysis of data obtained without any disturbers

It is assumed that the data can be related by an equation of the form

$$Nu = m\,(Re)^n$$

or $\log Nu = n \log Re + \log m$

The numbers n and m are found by the following equations

$$n = \frac{\sum_{m=1}^{S} \log Nu_m \left(\mathrm{Log}\, Re_m - \overline{\log Re}\right)}{\sum_{m=1}^{S} \left(\log Re_m - \overline{\log Re}\right)^2}$$

$$\log m = \overline{\log Nu} - n\,\overline{\log Re}$$

In these equations S is the total number of data points,

$$\overline{\log Re} = \frac{1}{S} \sum_{m=1}^{S} \log Re_m$$

and $$\overline{\log Nu} = \frac{1}{S} \sum_{m=1}^{S} \log Nu_m$$

Table (10) gives a summary of the terms obtained in the least square analysis of the data obtained for the 2 inch and 1 inch sections without any disturbers (Groups 1 and 6).

TABLE 10

RESULTS OF LEAST SQUARE ANALYSIS

Group No.	No. of Data Points	$\overline{\log Re}$	$\overline{\log Nu}$	n	m
1	21	4.5491	2.0357	0.547	0.343
6	21	4.6612	2.2199	0.580	0.328